Sequential, Divergent, and Cooperative Requirements of *Foxl2a* and *Foxl2b* in Ovary Development and Maintenance of Zebrafish

Yan-Jing Yang,*,† Yang Wang,* Zhi Li,* Li Zhou,*,[1] and Jian-Fang Gui*,[1]
*State Key Laboratory of Freshwater Ecology and Biotechnology, Institute of Hydrobiology, Chinese Academy of Sciences, and †Graduate University of the Chinese Academy of Sciences, Wuhan 430072, China

ABSTRACT *Foxl2* is essential for mammalian ovary maintenance. Although sexually dimorphic expression of *foxl2* was observed in many teleosts, its role and regulative mechanism in fish remained largely unclear. In this study, we first identified two transcript variants of *foxl2a* and its homologous gene *foxl2b* in zebrafish, and revealed their specific expression in follicular layer cells in a sequential and divergent fashion during ovary differentiation, maturation, and maintenance. Then, homozygous *foxl2a* mutants (*foxl2a*$^{-/-}$) and *foxl2b* mutants (*foxl2b*$^{-/-}$) were constructed and detailed comparisons, such as sex ratio, gonadal histological structure, transcriptome profiling, and dynamic expression of gonadal development-related genes, were carried out. Initial ovarian differentiation and oocyte development occur normally both in *foxl2a*$^{-/-}$ and *foxl2b*$^{-/-}$ mutants, but *foxl2a* and *foxl2b* disruptions result in premature ovarian failure and partial sex reversal, respectively, in adult females. In *foxl2a*$^{-/-}$ female mutants, *sox9a-amh/cyp19a1a* signaling was upregulated at 150 days postfertilization (dpf) and subsequently oocyte apoptosis was triggered after 180 dpf. In contrast, *dmrt1* expression was greater at 105 dpf and increased several 100-fold in *foxl2b*$^{-/-}$ mutated ovaries at 270 dpf, along with other testis-related genes. Finally, homozygous *foxl2a*$^{-/-}$/*foxl2b*$^{-/-}$ double mutants were constructed in which complete sex reversal occurs early and testis-differentiation genes robustly increase at 60 dpf. Given mutual compensation between *foxl2a* and *foxl2b* in *foxl2b*$^{-/-}$ and *foxl2a*$^{-/-}$ mutants, we proposed a model in which *foxl2a* and *foxl2b* cooperate to regulate zebrafish ovary development and maintenance, with *foxl2b* potentially having a dominant role in preventing the ovary from differentiating as testis, as compared to *foxl2a*.

KEYWORDS *Foxl2a*; *Foxl2b*; premature ovarian failure; sex reversal; TALEN

SEX is one of the most intriguing puzzles in biology since antiquity, and has been considered "the queen of problems in evolutionary biology" (Bell 1982; Bachtrog *et al.* 2014). Most animals reproduce sexually, but the mechanisms of sex determination (SD) and differentiation are remarkably varied (Marín and Baker 1998; Barske and Capel 2008; Bonduriansky 2009; Williams and Carroll 2009; Gui and Zhu 2012; Matson and Zarkower 2012). Sex-determining mechanisms in teleosts are rapidly evolving and highly plastic but usually depend on genetic factors, with interactions between genetic and environmental factors affecting downstream differentiation (Devlin and Nagahama 2002; Volff *et al.* 2007; Desjardins and Fernald 2009; Mei and Gui 2015; Li *et al.* 2016). Three distinct SD genes, *doublesex and mab-3 related transcription factor 1Y* (*Dmy/dmrt1bY*) (Matsuda *et al.* 2002), *gonadal somatic cell derived factor* (*gsdf*) (Myosho *et al.* 2012), and *sex-determining region Y* (*SRY*)*-box 3* (*sox3*) (Takehana *et al.* 2014), were respectively identified from three medaka species, *Oryzias latipes*, *O. luzonensis*, and *O. dancena*; suggesting that SD genes are diverse among different teleost species even in the same genus. An additional three SD genes—*anti-Mullerian hormone receptor type 2* (*amhr2*) in tiger pufferfish (*Takifugu rubripes*) (Kamiya *et al.* 2012), *Y-linked anti-Mullerian hormone* (*Amhy*) in silversides (*Odontesthes hatchery*) (Hattori *et al.* 2012), and *sexually dimorphic on the Y chromosome* (*sdY*) in rainbow trout (*Oncorhynchus mykiss*) (Yano *et al.* 2012)—were also

doi: https://doi.org/10.1534/genetics.116.199133
Manuscript received December 12, 2016; accepted for publication February 9, 2017; published Early Online February 13, 2017.
Supplemental material is available online at www.genetics.org/lookup/suppl/doi:10.1534/genetics.116.199133/-/DC1.
[1]Corresponding authors: Institute of Hydrobiology, Chinese Academy of Sciences, 7 Donghu South Rd., Wuhan 430072, Hubei, China. E-mail: jfgui@ihb.ac.cn; zhouli@ihb.ac.cn

identified as key factors to initiate testicular differentiation. During and after gonadal cell specification, germ cells and somatic cells mutually interact to coordinate sex differentiation of the gonads (Shinomiya *et al.* 2000; Devlin and Nagahama 2002; Siegfried and Nüsslein-Volhard 2008; Nishimura and Tanaka 2014). In most teleost species, ovarian differentiation begins with the proliferation of somatic cells and oogonia and early oocyte differentiation, while testicular differentiation usually occurs several weeks or months later than ovarian differentiation (Nakamura *et al.* 1998; Devlin and Nagahama 2002; Saito *et al.* 2007). In addition, sex in many fishes, even in some with heteromorphic sex chromosomes, is influenced or overrode by a variety of environmental and social cues, such as sex steroids, temperature, pH, salinity, density, hypoxia, and others (Baroiller *et al.* 2009; Desjardins and Fernald 2009; Mei and Gui 2015).

Zebrafish (*Danio rerio*), as a vertebrate model animal (Grunwald and Eisen 2002), has been well studied in the contexts of development and disease. Yet, its primary SD and differentiation mechanisms still remain controversial (Nagabhushana and Mishra 2016). Although differentiated sex chromosomes were not found in domesticated zebrafish strains (AB and TU) (Sola and Gornung 2001), a sex-determining region was recently demonstrated in wild zebrafish on a subtelomeric region of the long arm of chromosome *4* (Anderson *et al.* 2012; Howe *et al.* 2013; Wilson *et al.* 2014). Zebrafish sex may be determined by multiple genes, along with the influences of primordial germ cells and environmental factors (Liew and Orban 2013; Nagabhushana and Mishra 2016). The early gonadal development of zebrafish is a complicated process. All gonads initially develop as an undifferentiated "juvenile ovary," but approximately half of the ovarian tissues subsequently degenerate and transform into testicular tissue (Takahashi 1976). Although several key regulation genes—such as *SRY-box 9* (*sox9*); *nuclear receptor subfamily 5 group A* (*nr5a*); *cytochrome P450, family 19, subfamily A, polypeptide 1a* (*cyp19a1a*); *anti-Mullerian hormone* (*amh*); *GATA binding protein 4* (*gata4*); and *Wilms tumor 1* (*wt1*)—show sexually dimorphic expression patterns and are involved in zebrafish gonad differentiation (Chiang *et al.* 2001; Trant *et al.* 2001; Rodríguez-Marí *et al.* 2005; Von Hofsten and Olsson 2005; Jorgensen *et al.* 2008; Sreenivasan *et al.* 2008), it is unclear which of these or others might serve as the initiator(s) or master switch(es) for zebrafish SD and subsequent differentiation.

Forkhead (FKH) box (Fox) proteins which have a highly conserved 100 amino acid FKH DNA-binding domain (FHD), play specialized functions in many key biological processes (Carlsson and Mahlapuu 2002; Benayoun *et al.* 2011). Named after the *Drosophila melanogaster* gene *fork head* (*fkh*) (Weigel *et al.* 1989), >2000 family members have been identified in numerous species. Based on similarities in the FHD and unified nomenclature of *Fox* genes (Kaestner *et al.* 2000), Fox proteins are divided into 19 subfamilies, from FoxA to FoxS (Fetterman *et al.* 2008; Hannenhalli and Kaestner 2009). *Foxl2*, one of the earliest known markers of ovarian differentiation (Cocquet *et al.* 2002), is required for granulosa cell differentiation (Schmidt 2004) and to prevent transdifferentiation of an adult ovary to a testis by suppressing the SRY target gene *Sox9* (Uhlenhaut *et al.* 2009). *FOXL2* was first identified in blepharophimosis-ptosis-epicanthus inversus syndrome (BPES) patients with eyelid and craniofacial malformations (Crisponi *et al.* 2001). In addition, *FOXL2* mutation leads to premature ovarian failure (POF), a reduction in the number of germ cells in some BPES patients (De Baere *et al.* 2003; Meduri *et al.* 2010). In the *Foxl2* null mouse, granulosa cells fail to undergo the squamous-to-cuboidal transition, which leads to arrest of folliculogenesis and oocyte atresia (Schmidt 2004; Kocer *et al.* 2008). In teleosts, *foxl2* is expressed predominantly during ovary development of several species (Loffler *et al.* 2003), including Nile tilapia (*Oreochromis niloticus*) (Wang *et al.* 2004; Ijiri *et al.* 2008), rainbow trout (*O. mykiss*) (Baron 2004), dogfish (*Scyliorhinus canicula*) (Wotton *et al.* 2007), medaka (*O. luzonensis*) (Nakamoto *et al.* 2006), honeycomb grouper (*Epinephelus merra*) (Alam *et al.* 2008), wrasse (*Halichoeres trimaculatus*) (Kobayashi *et al.* 2010), African sharptooth catfish (*Clarias gariepinus*) (Sridevi and Senthilkumaran 2011; Bhat *et al.* 2016), and sablefish (*Anoplopoma fimbria*) (Smith *et al.* 2013). Additional studies have focused on associations of *foxl2* with aromatase and sex hormones in the brain-pituitary-gonad axis (Nakamoto *et al.* 2006; Nakamoto *et al.* 2007; Wang *et al.* 2007; Yamaguchi *et al.* 2007; Von Schalburg *et al.* 2010; Navarro-Martín *et al.* 2011; Sridevi and Senthilkumaran 2011; Sridevi *et al.* 2012; Crespo *et al.* 2013). Two *foxl2* homologous genes, *foxl2* and *foxl2-like*, have been identified in zebrafish (Crespo *et al.* 2013) and are referred to here as *foxl2a* and *foxl2b*, respectively, in accordance with their phylogenetic relationship and current naming conventions. The sexually dimorphic expression pattern of zebrafish *foxl2a* was already reported (Siegfried and Nüsslein-Volhard 2008; Siegfried 2010; Caulier *et al.* 2015), however, its functional role and regulative mechanism remained largely unclear and the expression pattern and function of *foxl2b* were completely unknown. Here, we characterized a sequential and divergent *foxl2a* and *foxl2b* expression in zebrafish. Using a transcription activator-like effector nucleases (TALEN) approach (Li *et al.* 2013; Ota *et al.* 2013; Huang *et al.* 2014), we constructed mutants for *foxl2a* and *foxl2b*, and identified cooperative roles for these genes in regulating ovary differentiation and maintenance.

Materials and Methods

Maintenance of fish

The wild-type (WT) zebrafish of strain AB was used to produce mutant lines. Embryos were produced by *in vitro* fertilization according to the protocol described in the zebrafish book (Westerfield 2007). Each group for expression analysis consisted of 30 mutants and 30 WT zebrafish, which was reared in recirculating freshwater tanks from 4 dpf at 28.5° on a

14 hr light/10 hr dark cycle (Westerfield 2007). All procedures were performed with the approval of the Animal Care and Use Committee of the Institute of Hydrobiology, Chinese Academy of Sciences.

Cloning and sequence analysis

Total RNAs were isolated at different stages using SV RNA Isolation Reagent (Promega, Madison, WI) and they were reverse transcribed with M-MLV Reverse Transcriptase (Invitrogen, Carlsbad, CA) at 37° with Oligo (dT) Primer. To ascertain or reexamine full-length complementary DNA (cDNA) sequences of *foxl2a* and *foxl2b*, a zebrafish oocyte SMART cDNA library was constructed according to the SMARTer PCR cDNA Synthesis Kit User Manual (Clontech). The *foxl2*a and *foxl2b* cDNAs were amplified by 3′ and 5′ RACE with primers (Supplemental Material, Table S1) designed according to the sequences in GenBank (NM_001045252.1 and XM_009298955.1). The complete cDNA sequences of *foxl2a-1*, *foxl2a-2*, and *foxl2b* were deposited in GenBank (accession numbers KR232688, KR232689, and KR232690, respectively).

Multiple amino acid sequence alignment was performed with the Clustal X program and refined with GeneDoc software. Phylogenetic analysis was performed with the Molecular Evolutionary Genetics Analysis (MEGA 5) software (Tamura *et al.* 2011) and the phylogenetic tree was constructed with neighbor-joining methods and 1000 bootstrap permutations. All the amino acid sequences used in the multiple alignment and phylogenetic analysis were obtained from GenBank (http://www.ncbi.nlm.nih.gov/) and RefSeq (http://www.ncbi.nlm.nih.gov/RefSeq/). The accession numbers are as follows: *Homo sapiens* FOXL2, NP_075555; *Mus musculus* FOXL2, NP_036150; *Gallus gallus* FOXL2, NP_001012630; *Chrysemys picta* FOXL2, XP_005282573; *O. niloticus* Foxl2, NP_001266707; *O. latipes* Foxl2, NP_001098358; *Salmo salar* Foxl2, XP_014018845; *O. mykiss* Foxl2, NP_001117957; *Cyprinus carpio* Foxl2, AKU47820; *Gobiocypris rarus* Foxl2, ADN38241; *D. rerio* Foxl2a, NP_001038717; *D. rerio* Foxl2b, NP_001304690; *Kryptolebias marmoratus* FoxL2, XP_017277495; *Fundulus heteroclitus* Foxl2, JAR75273; *Dicentrarchus labrax* Foxl2, ACW83540; *T. rubripes* Foxl2, XM_003968745; *Xenopus tropicalis* Foxl2, XP_004917868; *D. rerio* Foxl3, AAI62838; *T. rubripes* Foxl2-like, XP_011620275; *O. mykiss* Foxl3, NP_001117956; *S. salar* Foxl2-like, ADJ38819; *K. marmoratus* Foxl3, APD78564; *F. heteroclitus* Foxl2-like, XP_012705892; *D. labrax* Foxl3, AFV13295; *O. latipes* Foxl2-like, XP_004070713; *D. labrax* Foxl1, CBN81215; *D. rerio* Foxl1, NP_957278; *O. latipes* Foxl1, NP_001116391; *X. tropicalis* Foxl1, AAI35134; *G. gallus* FOXL1, XP_001231599; *H. sapiens* FOXL1, NP_005241; and *M. musculus* FOXL1, NP_032050. Syntenic analyses were carried out using information extracted from the Ensembl (http://www.ensembl.org) genome and the chromosomal regions around *foxl2s* genes in *H. sapiens* chromosome *3*, *M. musculus* chromosome *9*, *G. gallus* chromosome *9*, *X. tropicalis* chromosome *5*, and *D. rerio* chromosome *2* and chromosome *15* were assembled.

Quantitative RT- PCR

Quantitative RT-PCR (qRT-PCR) was performed on a DNA Engine Chromo4 Real Time System (Bio-Rad, Hercules, CA) with SYBR green qRT-PCR master mix (ToYoBo, Osaka, Japan) as described (Huang *et al.* 2009). All qRT-PCR reactions were performed in 20 μl reactions containing 10 μl 2× SYBR green master mix (Bio-Rad), 0.5 μl (10 μM) of each primer, 1 μl reverse transcriptase RT synthetic cDNA template, and 8 μl double distilled water. Samples were run with the following program parameters: 95° for 1 min, followed by 39 cycles of 95° for 15 sec, 60° for 30 sec, 76° for 5 sec, 79° for 5 sec, and 81° for 5 sec, ending with the melt curve 65–95°, with 0.5°/sec with each temperature lasting for 0.5 sec. Negative control (no-template DNA reaction) was always included. Specificity of amplification for each reaction was analyzed by dissociation curves using CFX manager software (Bio-Rad). To determine the optimal reference genes (Bustin *et al.* 2009), seven housekeeping genes—including *actin*, *β1* (*actb1*); *glyceraldehyde-3-phosphate dehydrogenase* (*gapdh*); *glucose-6-phosphate dehydrogenase* (*g6pd*); *TATA box binding protein* (*tbp*); *eukaryotic translation elongation factor 1 α1, like 1* (*eef1a1l1*); *polymerase* (*RNA*) *II* (*DNA directed*) *polypeptide D* (*polr2d*); and *succinate dehydrogenase complex*, *subunit A*, *flavoprotein* (*sdha*)—were selected to check their expression stability at the developmental stages and in the tissues analyzed. Rank ordering of expression stability using geNorm analysis (Vandesompele *et al.* 2002) identified *actb1* (*M* value = 1.387 < 1.5) and *sdha* (1.37) as the most stable normalizers during developmental stages and in the tissues analyzed, while *eef1a1l1* (1.805), *tbp* (1.839), *gapdh* (2.206), and *g6pd* (2.59) were the most variable. Therefore, *actb1* was selected as the normalizer for qRT-PCR in this study, and the relative expression levels of target genes were calculated using the $2^{-\Delta\Delta Ct}$ method (Livak and Schmittgen 2001). All the samples were analyzed in triplicates.

Probe synthesis and in situ hybridization

For antisense probe synthesis, T7 RNA polymerase promoter was added to the 5′ end of reverse primers and a DIG RNA Labeling Kit (Roche, Mannheim, Germany) was used. In brief, a 775-bp cDNA fragment of *foxl2a* and a 528-bp cDNA fragment of *foxl2b* were amplified by specific primers *foxl2a* probe N, *foxl2a* probe T7C, *foxl2b* probe N, and *foxl2b* probe T7C (Table S1). The ovarian tissues were fixed with 4% paraformaldehyde (PFA) in PBS at 4° overnight. After washing with PBS (pH 7.0) three times, the samples were immersed in 30% saccharose-PBS buffer overnight at 4°, then embedded in Optimal Cutting Temperature compound (Leica, Wetzlar, Germany) and sectioned to 10 μm in thickness using frozen microtomy (Leica, Wetzlar, Germany). After being dried at 37° for 1 hr, the cryostat sections were stored at −70°. Messenger RNA (mRNA) detection by sectioned tissue *in situ* hybridization (Stahl and Simon 2010) was performed as previously described (Yin *et al.* 2007). Images were acquired by Zeiss Axio Observer A1 inverted microscope (Leica).

TALEN design and assembly for foxl2a and foxl2b

The first exon sequences of *foxl2a* and *foxl2b* genomic loci from the Ensembl zebrafish genome browser were verified by PCR and sequencing. Potential TALEN target sites in the loci were searched using the TAL Effector Nucleotide Targeter (https://tale-nt-.cac.cornell.edu/) with the following parameters: (1) spacer length of 15–20, (2) repeat array length of 12 to 19, (3) T at position 0, and (4) a restriction enzyme cutting site in the spacer. Gene-specific TALEN constructs were assembled using the FastTALE TALEN Assembly Kit (Sidansai Biotechnology). The resulting arrays with TALEN backbones (left, pCS2-PEAS; and right, pCS2-PERR) were confirmed by sequencing.

Establishment of foxl2a and foxl2b mutant zebrafish lines

For *in vitro* transcription of these TALENs, pCS2-PEAS-*foxl2a*, pCS2-PERR-*foxl2a*, pCS2-PEAS-*foxl2b*, and pCS2-PERR-*foxl2b* were linearized with *NotI* and recovered as corresponding transcription templates. The transcriptions were carried out with the mMESSAGE and mMACHINE SP6 Kit (Ambion) and then quantified using NanoDrop-2000 (Thermo Scientific). The left arm and right arm mRNAs of each TALEN pair were mixed at a molar ratio of 1:1 before microinjection, and the mRNA mixtures with 200–600 pg final concentrations were directly microinjected into zebrafish embryos at the one-cell stage.

The injected embryos were hatched at 28.5°. At 24 hr after injection of TALEN mRNAs, genomic DNA (gDNA) was extracted from 20 randomly sampled embryos to evaluate the efficiency of TALEN-induced somatic mutations. The gDNA was obtained by the NaOH method (Meeker *et al.* 2007). The gDNA fragments including the target site of the TALENs were amplified using *foxl2a* and *foxl2b* gene-specific primers (Table S1). After digestion with *Bst*N I (restriction enzyme cutting site in the spacer of *foxl2a*) or *Bsr*D I (restriction enzyme cutting site in the spacer of *foxl2b*) (New England Biolabs, Beverly, MA) respectively at 60° and 65° for 2 hr, the uncleaved DNA fragments were separated by gel electrophoresis and cloned into pMD-18T vector (Promega). Sequence alignments were generated to analyze whether or not the gDNA fragments from embryos injected with TALEN mRNAs were mutated.

The F_0 founders carrying mosaic mutations were mated with WT zebrafish to generate heterozygous F_1 offspring. The heterozygous individuals with frameshift or nonsense sequence alterations in the F_1 generation were selected by fin-clip assay. Male and female siblings of the F_1 generation carrying the same mutation were mated to generate homozygous F_2 mutants as described previously (Xiong *et al.* 2017).

Sampling and histological examination

All fish sampled were anesthetized with MS-222 (tricaine methanesulfonate, 250 mg/l) (Sigma-Aldrich, St. Louis, MO) to measure body length and body weight. After the measurements, gonads of the fish were collected to calculate the gonadosomatic index (GSI) (gonadal weight/total body weight) values, and fixed in 4% PFA by overnight immersion. For histochemical analyses, 10-μm-thick sections were cut with frozen microtomy (Leica), stained with hematoxylin and eosin (Yulu, Nanchang, China), and mounted in neutral balsam (Sinopharm Chemical Reagent, Shanghai, China). Hematoxylin-eosin staining is performed as previously described (Xia *et al.* 2007). The slides were imaged by Zeiss Axio Observer A1 inverted microscope (Leica).

Transcriptome analysis

The ovaries from WT, *foxl2a*$^{-/-}$, and *foxl2b*$^{-/-}$ mutants at 150 dpf were sampled to isolate total RNA. Three biological replicates were analyzed per group. The transcriptome analysis, including library construction, sequencing, and bioinformatic analysis were performed by Beijing Genomics Institute, China. Briefly, after quality assessment by Agilent 2100 Bioanalyzer (Agilent Technologies) and agarose gel electrophoresis, the total RNAs were used to construct libraries. A narrow 400–450 bp size range was selected and enriched. The quantification and qualification of libraries were assessed by Agilent 2100 Bioanaylzer (Agilent Technologies) and ABI StepOnePlus Real-Time PCR System (Thermo Scientific). The flow cells amplified from qualified libraries on cBot were sequenced using the Illumina HiSeq 4000 System and 150-bp pair-end reads were generated. The assembly was performed with clean reads to produce the transcripts which were mapped to the Zv10 zebrafish genome for bioinformatic analysis. Differential expression profiles between WT and mutant samples were calculated using RSEM [RNA sequencing (RNAseq) by expectation maximization] (Li and Dewey 2011). The transcripts were classified according to the official annotation of the Gene Ontology (GO) Consortium, and the Kyoto Encyclopedia of Genes and Genomes (KEGG) enrichments were performed using phyper, a function of R. Statistical analysis of differentially expressed genes (DEGs) was performed using a relative change of ≥ 2 as the threshold to judge the significance of gene expression difference. False discovery rate (FDR) was used to determine the threshold of the *P*-value and GO or KEGG terms (FDR ≤ 0.01) were considered significantly enriched.

Statistical analysis

Statistical analyses were performed with SPSS (version 13.0) and OriginPro (version 8.0). All quantitative data were expressed as the mean ± SEM. Statistical analyses of the data were performed using an ANOVA, followed by Duncan's multiple range test. A probability of $P < 0.05$ was considered statistically significant.

Data availability

The DNA sequences have been deposited at National Center for Biotechnology Information (NCBI), accession numbers from KR232688 to KR232690. The raw data of transcriptomes have been submitted to the NCBI database (accession number: SRR4239959). See Table S2 for gene symbols, full names,

RefSeq identifications, and related references. All the Supplemental Table Legends have been shown in File S2.

Results

Molecular characterization of foxl2a and foxl2b in zebrafish

Similar to *foxl2a* transcripts (OTTDART00000051092 and OTTDART00000051093) in the Vertebrate Genome Annotation database (http://www.sanger.ac.uk/science/tools/vega-genome-browser), two transcript variants, named *foxl2a-1* (KR232688) and *foxl2a-2* (KR232689), were cloned from zebrafish ovary. Although the 5′ UTR sequences are different, they have an identical ORF (Figure 1A). The 5′ UTRs are transcribed from the first and second exon, respectively, suggesting that they arise from different transcriptional start sites. Moreover, *foxl2b* (KR232690) was also identified from zebrafish ovary (Figure 1B). The full-length cDNAs of *foxl2a-1*, *foxl2a-2*, and *foxl2b* are 1080, 1066, and 1269 bp, encoding 306, 306, and 285 amino acids, respectively. Similar to other vertebrate Foxl2 proteins, the FHD of zebrafish Foxl2a and Foxl2b are highly conserved, showing 98% amino acid identity, but their full amino acid sequences have only 64% identity (Figure S1 in File S1). Like other nonmammalian Foxl2 proteins, zebrafish Foxl2a and Foxl2b both lack glycine-rich (G), polyalanine tract (A), and proline-alanine-rich domains that are present in mammalian FOXL2 (Figure S1 in File S1). Phylogenetic analysis showed that vertebrate Foxl proteins were divided into three distinctive branches (Foxl1, Foxl2, and Foxl3). As shown in Figure 1, C and D, zebrafish Foxl2a and Foxl2b are both clustered into a Foxl2 grouping, indicating *foxl2* is duplicated in the zebrafish genome (Figure 1C) with paralogs on chromosomes *15* and *2*, respectively (Figure 1D). Other Foxl2-like genes are grouped with Foxl3, implying that they should be renamed as Foxl3 homologs. Although there is a highly conserved synteny within genomic regions of zebrafish, human, mouse, chicken, and frog around *foxl2* genes; a complementary loss/retention pattern exists in the vicinity genes of *foxl2a* and *foxl2b* between zebrafish chromosome *15* and chromosome *2* (Figure 1D), indicating that they might undergo divergent evolution after duplication.

Sexually dimorphic expression between adult gonads and sequential and divergent expression of foxl2a and foxl2b during ovary development

First, sexually dimorphic expression of *foxl2a* and *foxl2b* was observed by qRT-PCR in zebrafish mature ovaries and testes. As shown in Figure 2A, *foxl2a-1*, *foxl2a-2*, and *foxl2b* were all expressed in mature ovaries, whereas their expression was almost absent in mature testes. Then, we analyzed their expression levels during ovary differentiation, maturation, and maintenance. As shown in Figure 2B, *foxl2a* including *foxl2a-1* and *foxl2a-2* initiated expression early during ovary differentiation, and quickly reached peak values at 45 dpf (*foxl2a-1*) and 35 dpf (*foxl2a-2*), respectively. By contrast, *foxl2b* expression was relatively lower and gradually increased through the early stages of ovary differentiation from 15 to 45 dpf. Then, coinciding with diminishing expression of *foxl2a-1* and *foxl2a-2*, *foxl2b* expression increased and reached a peak at 105 dpf, and then remained at a relative high level in the mature ovary and stages of oocyte maintenance (Figure 2B).

The cellular localization and spatio-temporal distribution of *foxl2a* and *foxl2b* were assessed in ovaries at 35 and 105 dpf by *in situ* hybridization on tissue sections. Both *foxl2a* and *foxl2b* were expressed in follicular layer cells (FLCs) around the primary-growth oocytes (POs) in 35 dpf ovary, and *foxl2a* transcript signal was stronger than *foxl2b* (Figure 2C). At 105 dpf, *foxl2a* transcript was mainly localized in FLCs around POs, previtellogenic oocytes (PVOs), and vitellogenic oocytes (VOs), and its signal became very weak in mature oocytes (MOs) (Figure 2D). In contrast, *foxl2b* transcript was ubiquitously localized in FLCs around all oocytes (POs, PVOs, VOs, and MOs), and became stronger in MOs at 105 dpf ovary (Figure 2D). Therefore, *foxl2a* is expressed in early FLCs and may function early in ovary development, whereas *foxl2b* may function later.

Establishment of foxl2a and foxl2b knockout mutant lines

To explore the function of *foxl2a* and *foxl2b* in zebrafish SD and differentiation, we constructed two homozygous mutant lines, *foxl2a*$^{-/-}$ and *foxl2b*$^{-/-}$, by using TALEN. The TALEN target sites near the translation start codon were chosen to disrupt the translation of Foxl2a and Foxl2b proteins (Figure 3, A and B). Specific primers were designed to amplify a *foxl2a* or *foxl2b* DNA fragment containing the TALEN target site and a cleavage site with *Bst*N I or *Bsr*D I, respectively (Figure 3, A and B). A 523-bp DNA fragment of *foxl2a* amplified from WT embryos was completely digested by *Bst*N I to produce two DNA fragments (307 and 216 bp), while the fragments from TALEN F_0 embryos could not be completely digested (Figure 3C). This suggested that F_0 embryos were chimeric for modification of the *Bst*N I site. Indeed, a total of eight different indels modified at the target site were found from 20 embryos (Figure 3E), and the mutation frequency in F_0 founders was ~70% (14/20). Similarly, *foxl2b* was also successfully disrupted by the TALEN approach (Figure 3, D and F), and the mutation rate was 66.7% (8/12) in the F_0 founders (Figure 3F).

Subsequently, the remaining F_0 embryos were raised to adulthood and crossed with WT zebrafish. PCR amplification and digestion were done with gDNA of F_1 embryos to test for germ line transmission of induced lesions. Since the 5-bp deletion (Δ5) in *foxl2a* leads to a frameshift, it was chosen to be crossed with WT zebrafish to obtain F_1 offspring. Sibling F_1 male and female individuals carrying the same mutation were crossed with each other to produce homozygous F_2 mutants (*foxl2a*$^{-/-}$) whose genotypes were also confirmed by PCR amplification and digestion. The PCR-amplified fragment from homozygous *foxl2a*$^{-/-}$ F_2 mutants could not be

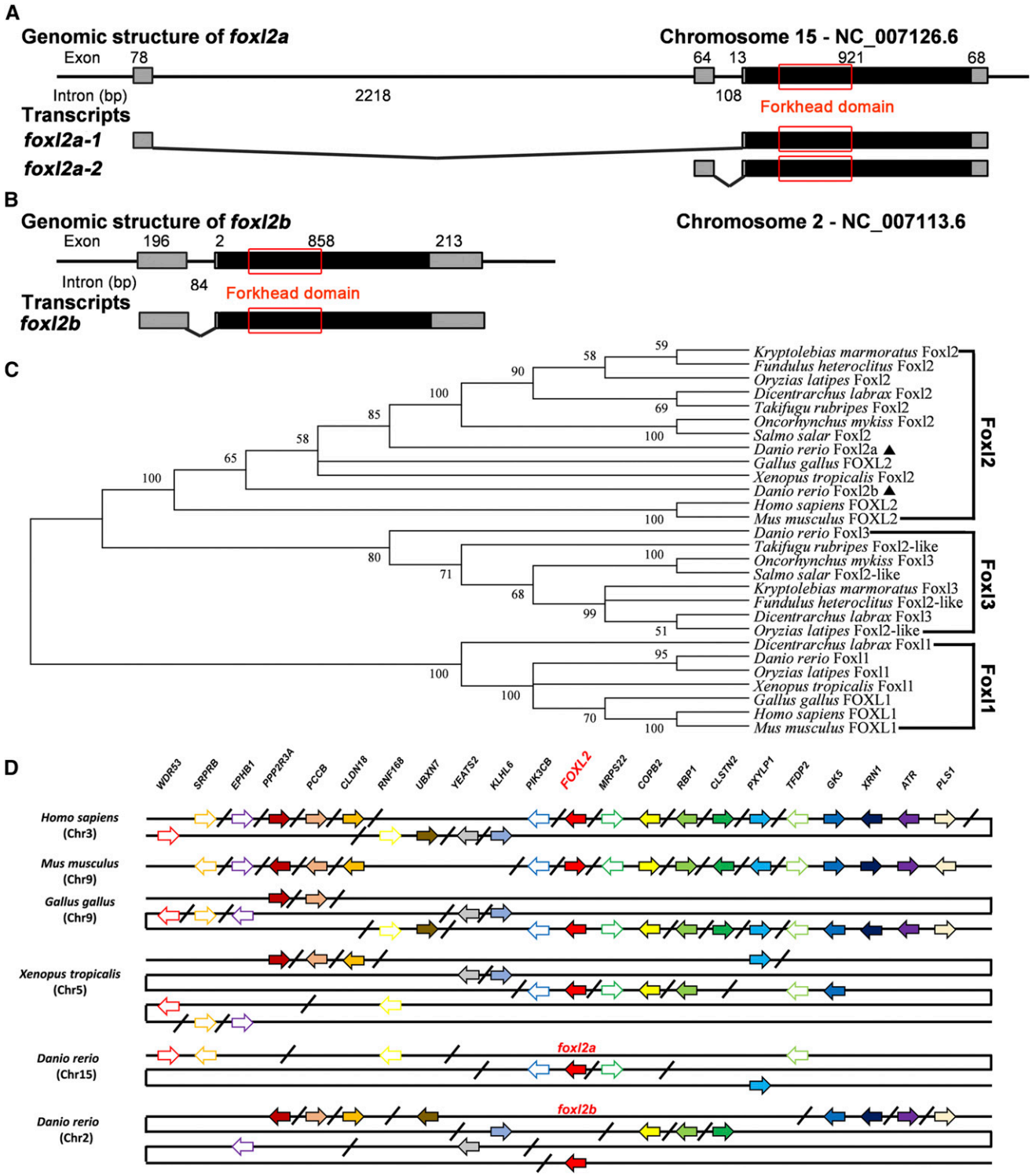

Figure 1 Molecular characterization of zebrafish *foxl2a* and *foxl2b*. (A and B) Genomic structure and transcript schematics of zebrafish *foxl2a* and *foxl2b*. Exons and introns are shown by boxes and horizontal lines, respectively. ORFs and FHD are highlighted by black boxes and red boxes, respectively. The exon and intron size are indicated above or below as bp. (C) Phylogenetic tree of Foxl proteins in vertebrates. (D) Syntenic alignment of chromosomal regions around vertebrate *foxl2* genes. Zebrafish *foxl2a* and *foxl2b* are located on chromosome *15* and *2*, respectively. Chromosome segments are represented as thick lines. The conserved gene blocks are shown in matching colors and the transcription orientation are indicated by arrows. The oblique line between two genes shows their discontinuity. Gene symbols, full names, RefSeq identifications, and related references are listed in Table S2. Chr, chromosome.

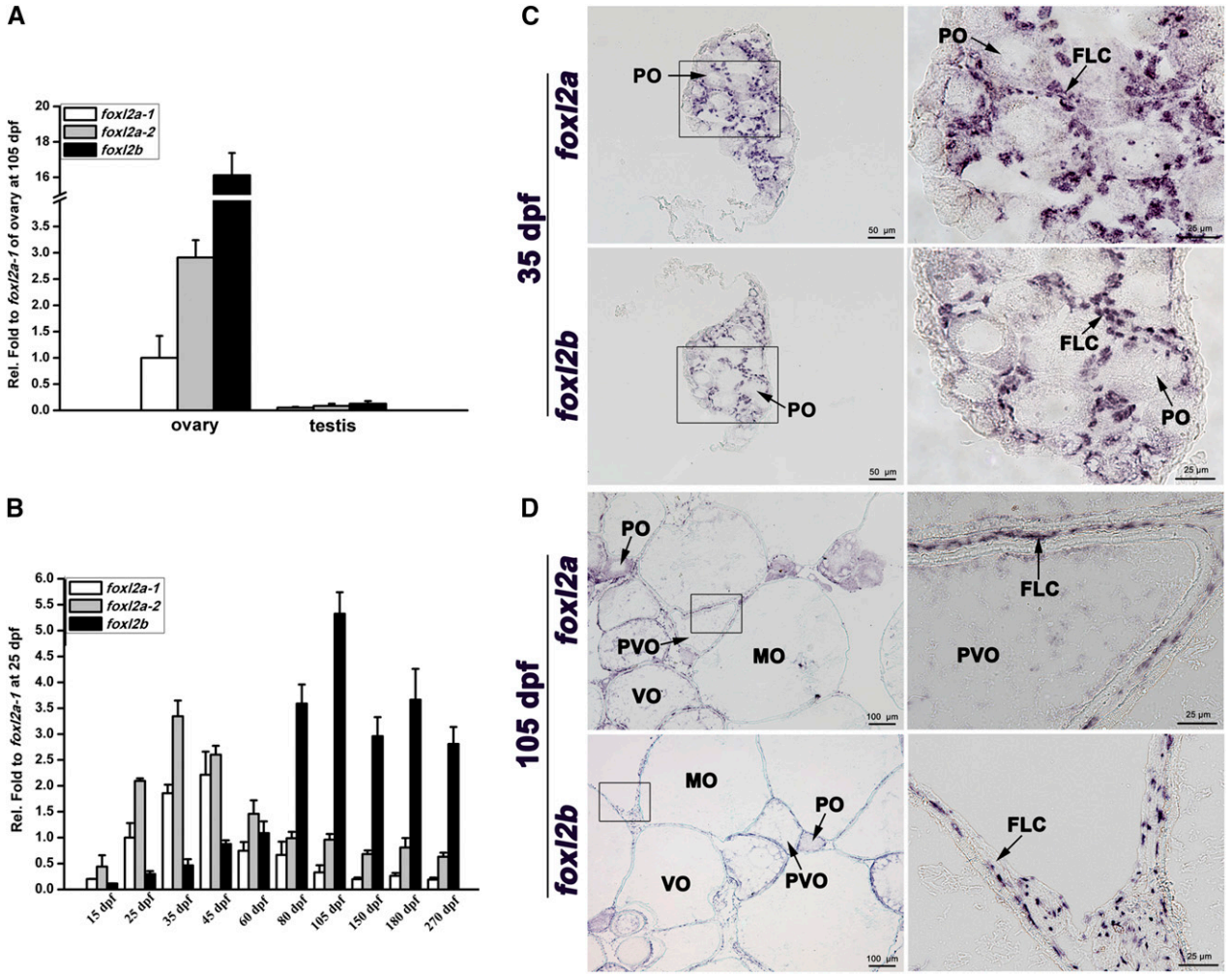

Figure 2 Expression characterization of zebrafish *foxl2a-1*, *foxl2a-2*, and *foxl2b* during ovary development and maintenance. (A) Sexually dimorphic expression between mature ovary and testis. (B) Sequential and divergent expression during ovary development and maintenance from 15 to 270 dpf. The qRT-PCR quantification of gene expression was normalized to *actb1*. The relative expression values were first calculated against *actb1* and then against that of *foxl2a-1* at 25 dpf. (C and D) Ovary section *in situ* localization at (C) 35 dpf and (D) 105 dpf. Bars are shown at bottom-right of the images.

digested by *Bst*N I (Figure 3C). Similarly, a 23-bp deletion (Δ23) in *foxl2b* leading to frameshifting of the coding sequence was also selected to successfully establish the *foxl2b* mutant line (*foxl2b*$^{-/-}$) (Figure 3, D and F). To confirm successful deletion in *foxl2a* and *foxl2b* genes, RT-PCR analyses were performed to ensure no expression of functional transcripts. Indeed, no WT transcripts were detected in the mutant ovaries by using the specific primers over the deleted sequences of *foxl2a*$^{-/-}$ (Δ5) and *foxl2b*$^{-/-}$ (Δ23) (Figure 3G).

Foxl2a deficiency leads to POF in adult females

To explore the function of *foxl2a* and exclude the effects of environmental factors on zebrafish SD and differentiation, we raised to adulthood 30 homozygous *foxl2a*$^{-/-}$ F_3 individuals and 30 control individuals together in one aquarium with 6 replicates. Zebrafish females began to spawn around 3 months after hatching in our aquarium system. The gross morphology and histology of the ovaries were analyzed both in the controls (WT) and homozygous mutants (*foxl2a*$^{-/-}$). It was difficult to identify mutants by body size and shape (Figure 4), so we randomly sampled individuals (including mutants and controls) at different ages to identify genotype and sex. As shown in Figure S2 in File S1, *foxl2a*$^{-/-}$ mutants and controls both had a normal 1:1 sex ratio. At 35 dpf, zebrafish gonads could be distinguished as either an ovary or a testis by morphology under dissection microscope. Histological analyses showed that the gonads of *foxl2a*$^{-/-}$ female mutants contained numerous POs, similar to controls (Figure S3 in File S1). At 60 dpf, some oocytes of both *foxl2a*$^{-/-}$ mutants and controls started to enter the PVO and VO stage (Figure S3 in File S1). This indicates that initial ovarian differentiation and oocyte development occur normally in *foxl2a*$^{-/-}$ mutants. At 105 dpf when adult fishes were ready for spawning, the ovaries from *foxl2a*$^{-/-}$ mutants and controls both contained large numbers of POs, PVOs, VOs, and

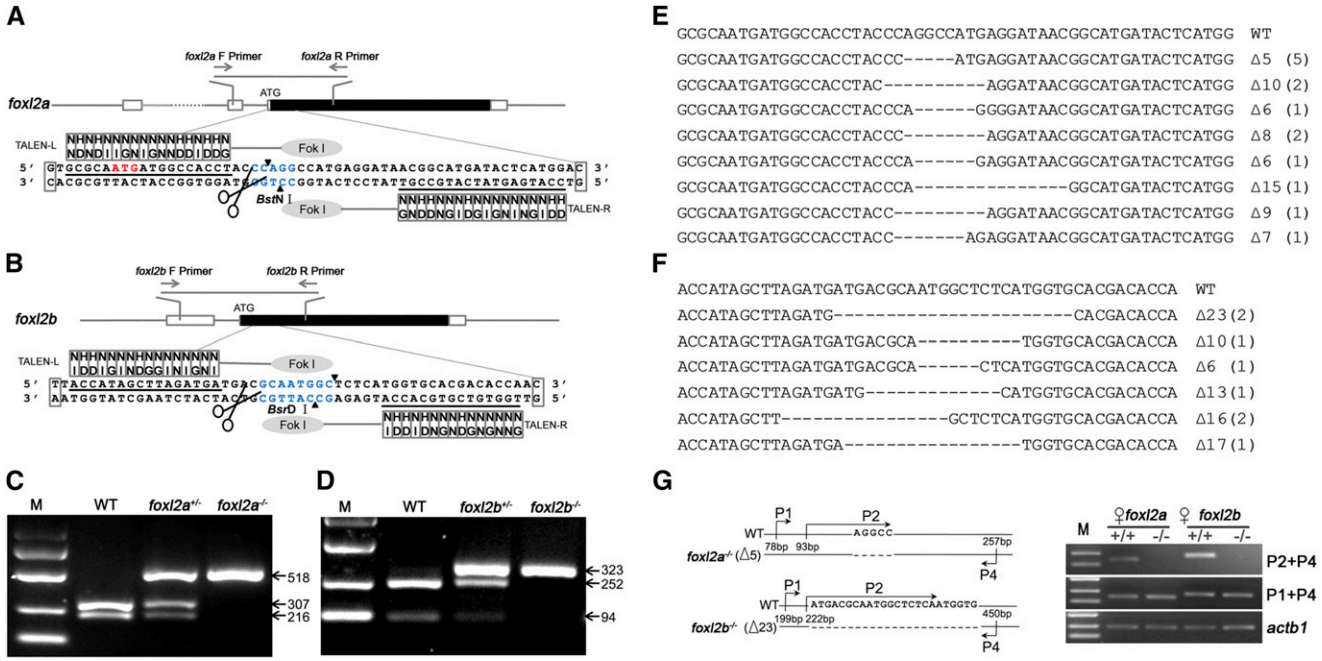

Figure 3 Establishment of *foxl2a* and *foxl2b* knockout mutant lines by TALEN. (A and B) The TALEN target sites of zebrafish (A) *foxl2a* and (B) *foxl2b*. The coding and untranslated exon regions are depicted as solid and open boxes, respectively. The left and right TALEN binding sites are indicated by underlining. Cleavage sites with *Bst*N I and *Bsr*D I in the spacer are shown by blue color, and forward and reverse primers (F primer and R primer) are indicated in the corresponding sites. (C and D) Detection of (C) *foxl2a* and (D) *foxl2b* mutants by *Bst*N I or *Bsr*D I digestion. The amplified fragment sizes (bp) are shown on the right. (E and F) Sequences of different indels of TALEN-induced (E) *foxl2a* and (F) *foxl2b* mutants in F_0 embryos. A total of eight and six indels (number of embryos are indicated in each bracket) at targeted locus are shown for (E) *foxl2a* and (F) *foxl2b*, and the numbers at the right-hand side indicate the number of deleted base pairs. (G) Transcription-level confirmation of *foxl2a* and *foxl2b* mutants by RT-PCR. The detected primers are shown on the left, and primer P2 is specific for the deleted sequences. The *actb1* was used as control. F, forward; R, reverse; M, marker.

MOs (Figure 4A). The results indicate that *foxl2a*$^{-/-}$ female mutants exhibit normal ovarian differentiation and oocyte development.

Considering POF in some human BPES patients with *FOXL2* mutation, we continued to raise *foxl2a*$^{-/-}$ mutants and controls together after spawning, and examined the status of ovaries during later adult life. Because ovulation occurs asynchronously, zebrafish can spawn continuously after maturation. Oocytes of both *foxl2a*$^{-/-}$ mutants and controls were recruited into maturation and ovulated again at 150 dpf (Figure 4B). In contrast to controls, for which all females spawned again, ~10 and 60% of *foxl2a*$^{-/-}$ female mutants with enlarged abdomens failed to spawn again at 180 and 270 dpf, respectively. Dissection showed that the ovaries of *foxl2a*$^{-/-}$ mutants became white at 180 dpf, and a large number of somatic cells filled in the lobules of ovarian tissues (Figure 4C). No oocytes at the previtellogenic and vitellogenic stages were observed, and only some degenerating primary-growth oocytes (DPOs) and degenerating oocytes (DOs) existed in the edges of each lobule (Figure 4C). Along with oocyte failure, the ovaries of *foxl2a*$^{-/-}$ mutants became transparent and aggravated, and only a few DPOs and vestiges of DOs were retained in lobules full of proliferating somatic cells (Figure 4D). In contrast, control individuals could persistently spawn, and the ovaries still contained POs, PVOs, VOs and MOs at 180 and 270 dpf (Figure 4, C and D). Although equal GSI values were observed among all the analyzed females at 105 and 150 dpf, the GSI values of *foxl2a*$^{-/-}$ females were much lower than those of WT females at 180 and 270 dpf (Figure 4E) ($P < 0.05$). The accelerated ovarian aging and oocyte failure in *foxl2a*$^{-/-}$ mutants are very similar to POF in human patients (Pal and Santoro 2002), suggesting that zebrafish *foxl2a* might also play a similar role in regulating ovarian senescence like its homologous gene in humans.

Foxl2b disruption results in partial sex reversal in adult females

Similarly, we also raised 30 homozygous *foxl2b*$^{-/-}$ F_3 individuals and 30 control individuals together in one aquarium with six repeats. *Foxl2b*$^{-/-}$ mutants and controls both had normal 1:1 sex ratios from 35 to 150 dpf (Figure S2 in File S1). In contrast to control females that all spawned again, ~20 and 70% of *foxl2b*$^{-/-}$ female mutants failed to spawn again at 180 and 270 dpf, respectively (Figure S2 in File S1 and Figure 5). In addition, the secondary sexual characteristics of these *foxl2b*$^{-/-}$ female individuals progressively transformed from those of males to females. At 105 and 150 dpf, these females still manifested typical secondary feminine characteristics, having a round and bluish body with a large visible urogenital papilla and an indistinct anal fin coloration (Figure 5, A and B). From 180 dpf, some *foxl2b*$^{-/-}$ females

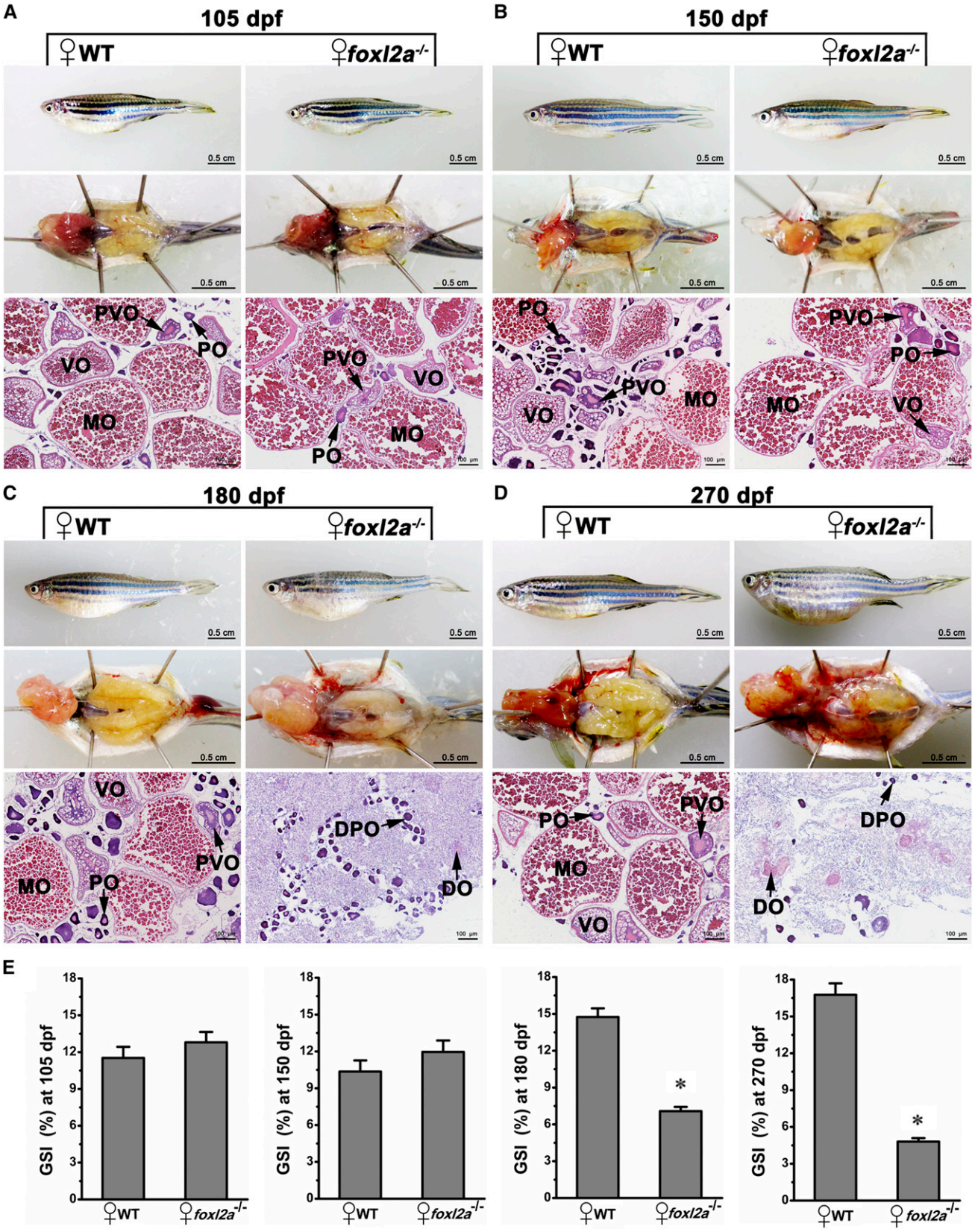

Figure 4 Disruption of *foxl2a* leads to similar POF in adult females. (A–D) Gross morphology, anatomical, and histological examination of adult ovaries in WT controls and *foxl2a* mutants (*foxl2a*$^{-/-}$) were analyzed at (A) 105 dpf (n = 12), (B) 150 dpf (n = 6), (C) 180 dpf (n = 3), and (D) 270 dpf (n = 6). (E) GSI values in control females and *foxl2a* mutant females. Data are presented as mean ± SEM * $P \leq 0.05$ (Duncan's multiple range test). Bars are shown at bottom right of the images. ♀, female; ♂, male.

exhibited mixed secondary sexual characteristics, including a slim and reddish body, an anal fin with distinct markings and a feminine urogenital papilla (Figure S4C in File S1). This implies that the homozygous *foxl2b*$^{-/-}$ female mutants undergo sex change after maturation. To further investigate the sex in *foxl2b*$^{-/-}$ females, the ovaries were sectioned for histological analyses. The ovaries of these mutants became transparent or white and exhibited partial sex reversal with different proportions of degenerating ovarian tissue and newborn testicular structure (Figure 5, C and D). At 180 dpf, lobules contained numerous somatic cells, with DPOs and vestiges of DOs scattered in the early transitional gonads (Figure 5, C and E). Along with the process of sex reversal, some similar spermatogenic cysts (SCs) containing spermatogonia (SG), spermatocytes (SPs), and spermatids emerged at 270 dpf, and a few of vestiges of DOs were still retained in the lobules (Figure 5, D and F). However, the female *foxl2b*$^{-/-}$ mutants did not completely change to fertile males, and gradually died off after 270 dpf, likely owing to hyperplasia of testicular and kidney tissues. Meanwhile, the GSI values of *foxl2b*$^{-/-}$ females in the process of sex reversal decreased more sharply than those of WT females from 180 to 270 dpf (Figure 5G) ($P < 0.05$). Therefore, *foxl2b* might play different roles in regulating ovary development and maintenance as compared to *foxl2a*.

Transcriptome profiling comparisons of initial transformation ovaries in foxl2a$^{-/-}$ *or foxl2b*$^{-/-}$ *females relative to normal ovaries in control females*

To reveal the pathways or genes influenced early by *foxl2a* or *foxl2b* deficiency, we performed comparative transcriptome analyses to investigate DEGs between initial transformation ovaries in *foxl2a*$^{-/-}$ mutants, or *foxl2b*$^{-/-}$ mutants and normal ovaries at the same age. In mice, Foxl2 cooperates with estrogen receptor 1 (ESR1) to repress *Sox9* expression (Uhlenhaut *et al.* 2009). Before transcriptome analyses, we first tested whether this pathway was conserved in zebrafish by evaluating *sox9a* expression changes at 150 dpf, because significant changes in gonad histology had occurred at 180 dpf, even though no apparent abnormalities were observed at 150 dpf (Figure 4B and Figure 5B). Indeed, the expression of *sox9a* was up-regulated both in *foxl2a*$^{-/-}$ and *foxl2b*$^{-/-}$ mutant ovaries at 150 dpf (Figure S5 in File S1), indicating that the gonadal transformation process had already been initiated. Therefore, the ovary at 150 dpf is suitable for performing RNAseq analysis. After filtration to remove the reads with low quality or adaptors, ~30,000,000 clean reads in each sample were obtained and assembled into ~23,000 transcripts (Table S3). In comparison with control ovaries, a total of 6005 and 6253 DEGs were respectively revealed in *foxl2a*$^{-/-}$ and *foxl2b*$^{-/-}$ ovaries at 150 dpf (Table S4), in which 1220 and 1314 DEGs were both upregulated or downregulated in *foxl2a*$^{-/-}$ and *foxl2b*$^{-/-}$ mutant ovaries (Figure S6A in File S1 and Table S4). The pathway with most annotated unigenes of commonly upregulated DEGs in KEGG was the "TNF signaling pathway," followed by "cytokine-cytokine receptor interaction" (Figure S6B in File S1 and Table S5), indicating the pathways involved in apoptosis or necroptosis were activated in both *foxl2a*$^{-/-}$ and *foxl2b*$^{-/-}$ mutant ovaries. In contrast, three pathways in "lipid metabolism" were found in the top 10 enriched KEGG pathways of commonly downregulated DEGs, implying the lipid synthesis or secretion was suppressed in both *foxl2a*$^{-/-}$ and *foxl2b*$^{-/-}$ mutant ovaries compared to control ovaries (Figure S6C in File S1 and Table S5).

To reveal differential regulation by *foxl2a* and *foxl2b*, the DEGs specifically changed in *foxl2a*$^{-/-}$ and *foxl2b*$^{-/-}$ mutant ovaries were respectively analyzed. As shown in Figure S6A in File S1, a total of 4471 and 3719 unigenes changed their expression levels in *foxl2a*$^{-/-}$ and *foxl2b*$^{-/-}$ mutant ovaries compared to control ovaries. The KEGG mapping analysis showed the differentially enriched pathways between these DEGs (Figure S6, D–G, in File S1; Table S5). Among the top 20 enriched pathways, only one pathway ("neuroactive ligand-receptor interaction") was shared between specifically upregulated DEGs from *foxl2a*$^{-/-}$ and *foxl2b*$^{-/-}$ mutant ovaries. Significantly, several important gonadal development-related genes (*e.g.*, *sox9a*, *wt1*, *gata4*, *sox3*, and *nr5a2*) and *foxl2b* were specifically upregulated in *foxl2a*$^{-/-}$ mutant ovaries, while *dmrt1* and *sox9b* were upregulated in *foxl2b*$^{-/-}$ mutant ovaries (Table S4).

Dynamic expression changes of gonadal development-related genes in foxl2a$^{-/-}$ *or foxl2b*$^{-/-}$ *female mutants during gonad transformation*

In consideration of the significant gonad transition that occurred in *foxl2a*$^{-/-}$ or *foxl2b*$^{-/-}$ female mutants (Figure 4 and Figure 5), we selected several genes involved in gonadal development (Table S4, Table S5, and Figure 6A) to further confirm their dynamic expression changes by using qRT-PCR analyses in transforming gonads from 105 to 270 dpf (Figure 6, B–N). This analysis revealed differential modulation of gene expression between *foxl2a*$^{-/-}$/WT and *foxl2b*$^{-/-}$/WT ovaries from 105 to 270 dpf. As expected, *sox9a* expression started to rise after the sexual maturity in *foxl2a*$^{-/-}$ female mutants at 105 dpf, and gradually increased up to 12-fold at 270 dpf. In contrast, the expression of *sox9a* rose at 150 dpf and increased up to 92-fold in *foxl2b*$^{-/-}$ female mutants against that of control ovaries at 270 dpf (Figure 6B). As a downstream target of *sox9a*, *amh* expression started to rise after *sox9a* increase (150 dpf) and reached a peak with a 10-fold increase at 180 dpf in *foxl2a*$^{-/-}$ mutants, while it maintained a low expression level until 180 dpf and increased dramatically (2255-fold) in expression at 270 dpf in *foxl2b*$^{-/-}$ female mutants (Figure 6C). *cyp19a1a* gradually decreased in abundance in both *foxl2a*$^{-/-}$ and *foxl2b*$^{-/-}$ female mutants, but the downward trend was more violent in latter (Figure 6D). Consistent with oocyte apoptosis and degeneration in *foxl2a*$^{-/-}$ and *foxl2b*$^{-/-}$ mutants, the expression of apoptosis-related genes *casp8* and *tnfrsf1a* gradually increased from 105 dpf. These data support the possibility that the upregulation of *sox9a-amh/cyp19a1a*

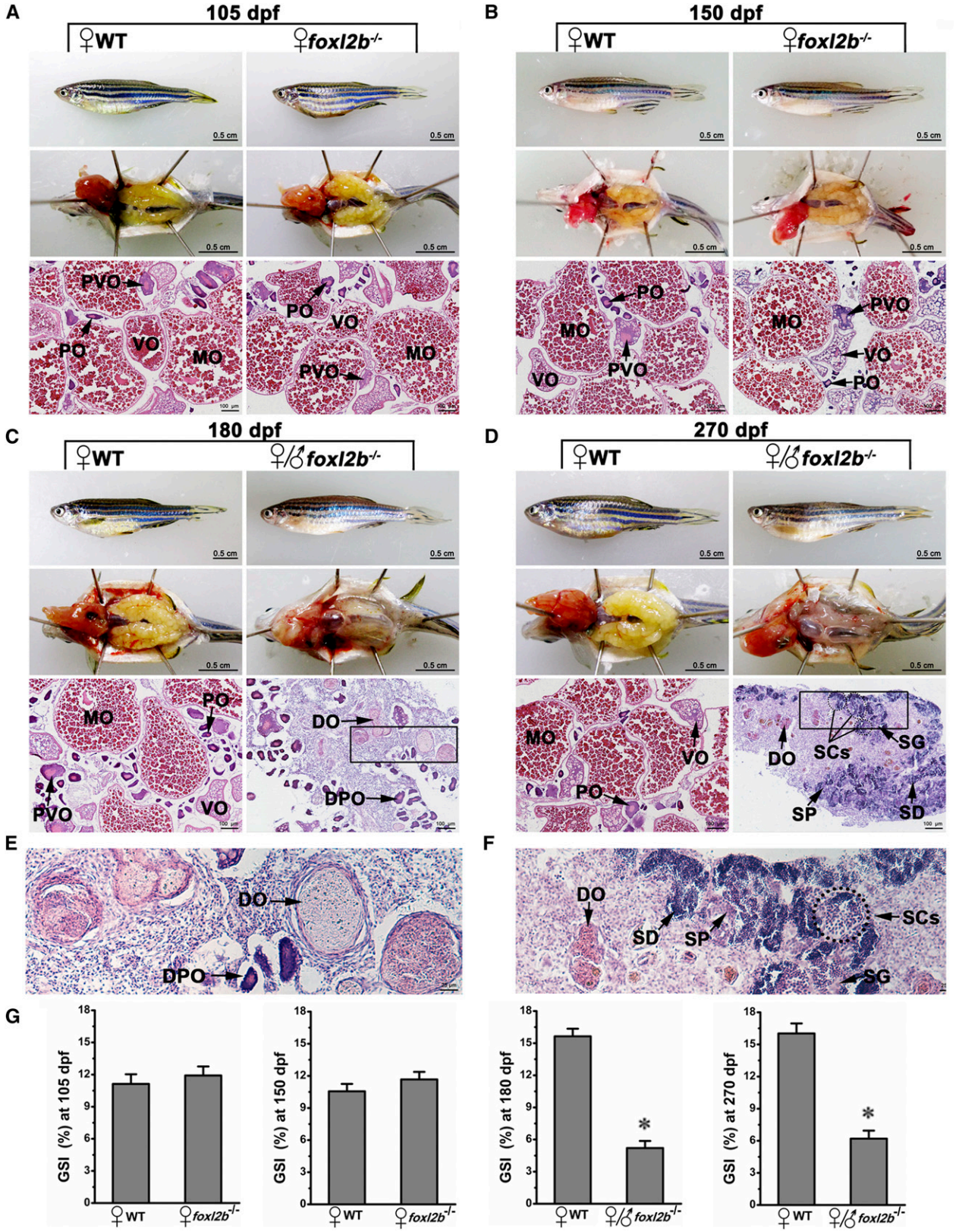

Figure 5 Partial sex reversal toward testicular tissue in *foxl2b*-deficient adult females. (A–F) Gross morphology, anatomical, and histological examination of adult ovaries in controls (WT) and *foxl2b* mutants (*foxl2b*$^{-/-}$) were analyzed at (A) 105 dpf (n = 13), (B) 150 dpf (n = 6), (C) 180 dpf (n = 5), and (D) 270 dpf (n = 7). Higher magnifications of the boxed areas in (C) and (D) are shown in (E) and (F). (G) GSI values in control females and *foxl2b* mutant females. Data are presented as mean ± SEM * $P \leq 0.05$ (Duncan's multiple range test). ♂, female; ♀, male; SD, spermatid. Bars are shown at bottom right of the images.

signaling triggers oocyte apoptosis and degeneration in both female *foxl2a*$^{-/-}$ mutants and *foxl2b*$^{-/-}$ mutants. Interestingly, the dynamic expression changes in *foxl2b*$^{-/-}$ mutants showed a delayed pattern compared to *foxl2a*$^{-/-}$ mutants (Figure 6, B–F), suggesting a transition in functional requirements from *foxl2a* to *foxl2b* at later stages.

Compared to that in corresponding control ovaries, testis differentiation-related genes, such as *dmrt1*, *wt1a*, *gata4*, *nr5a2*, and *nr5a5*, maintained a moderately increased expression in ovaries of *foxl2a*$^{-/-}$ mutants, while their expression in *foxl2b*$^{-/-}$ mutants increased dramatically from dozens to several 100-fold at 270 dpf (Figure 6, G–K), consistent with the sex change that occurred in *foxl2b*$^{-/-}$ mutants (Figure 5). Although *nr5a1b* expression was not significantly different in ovaries between the female controls and *foxl2a*$^{-/-}$ mutants, it also increased by ~69-fold at 270 dpf in the ovotestis of *foxl2b*$^{-/-}$ mutants (Figure 6L). These results suggest that *foxl2a* and *foxl2b* might play some divergent roles in regulating ovary development and maintenance, where *foxl2b* is specific for inhibiting testis development.

Besides the degeneration of oocytes, the massive increase of somatic cells (Figure 4, C and D) indicates that a POF might have occurred in *foxl2a*-deficient female zebrafish. Both germ cell marker genes *piwil1* and *dazl* expression levels in *foxl2a*$^{-/-}$ mutant ovaries were equal to those of control ovaries at 105 and 150 dpf. However, they sharply decreased in abundance to 11 and 24% at 270 dpf, respectively (Figure 6, M and N), indicating that the germ cells largely reduce in *foxl2a*$^{-/-}$ mutant ovaries from 180 dpf. In contrast, *piwil1* and *dazl* expression in *foxl2b*$^{-/-}$ female mutants increased in ovotestis at 270 dpf (Figure 6, M and N). This is probably due to a large number of spermatogenic cysts that contain male germ cells generated during gonad transformation from ovary to testis. Additionally, nine *cytochrome P450* (*cyp*) genes also showed differential modulation of gene expression between *foxl2a*$^{-/-}$/WT and *foxl2b*$^{-/-}$/WT ovaries from 105 to 270 dpf (Figure 7), indicating that both *foxl2a* and *foxl2b* regulate the steroidogenesis in zebrafish gonads, and their effects on steroid homeostasis differ.

Simultaneous disruption of foxl2a and foxl2b leads to complete sex reversal

Owing to the high identity in amino acid sequence and the sequential and divergent expression between *foxl2a* and *foxl2b*, we speculated that their functions would be compensatory in some ways. To address this, zebrafish homozygous *foxl2a/foxl2b* F_2 double mutants (*foxl2a*$^{-/-}$/*foxl2b*$^{-/-}$) carrying Δ5 in *foxl2a* and Δ23 in *foxl2b* were created. One-cell embryos were co-injected as described above with the two TALEN mRNAs which caused *foxl2a* mutation or *foxl2b* mutation, respectively. The heterozygous *foxl2a*$^{+/-}$/*foxl2b*$^{+/-}$ double mutant individuals were chosen to cross with each other. In the examined 11 homozygous double mutant individuals with *foxl2a*$^{-/-}$/*foxl2b*$^{-/-}$ genotype from the crossing, interestingly, only mature males with normal testis (Figure S7 in File S1) were found, whereas no adult females were observed. To acquire more homozygous *foxl2a*$^{-/-}$/*foxl2b*$^{-/-}$ mutants, we raised offspring of *foxl2a*$^{-/-}$/*foxl2b*$^{+/-}$ (female) crossed with *foxl2a*$^{-/-}$/*foxl2b*$^{-/-}$ (male) in one aquarium. At 105 dpf, a total of 45 individuals were randomly sampled to examine their genotypes and gonads, and 24 individuals were identified as homozygous *foxl2a*$^{-/-}$/*foxl2b*$^{-/-}$. In comparison with normal gonads in *foxl2a*$^{-/-}$/*foxl2b*$^{+/-}$ female and male adults (11 females and 10 males) (Figure 8A), again, no mature females with normal ovaries were observed. Only males were detected from the 24 homozygous *foxl2a*$^{-/-}$/*foxl2b*$^{-/-}$ adults, of which three individuals showed dual secondary sexual characteristics, such as feminine urogenital papilla and masculine anal fin (Figure S2 and Figure S4D in File S1), and abnormal ovotestis with DPOs and DOs as well as numerous SCs containing SG, SPs, and spermatids (Figure 8B). Another 21 individuals were found to have normal secondary masculine characteristics, including a nonvisible papillae, a slim and reddish body, and a big anal fin with distinct markings (Figure S4D in File S1), and normally developed testis full of SG, SPs and spermatids (Figure 8B). GSI values of homozygous *foxl2a*$^{-/-}$/*foxl2b*$^{-/-}$ females with sex reversal characteristics were much lower than those of heterozygous *foxl2a*$^{-/-}$/*foxl2b*$^{+/-}$ females at 105 dpf (Figure 8C) ($P < 0.05$).

To investigate when *foxl2a/foxl2b* deficiency affects ovary development and leads to sex reversal, we checked the gonadal development status of homozygous *foxl2a*$^{-/-}$/*foxl2b*$^{-/-}$ individuals from young to adults at 35, 40, 50, 60, 105, and 150 dpf. As shown in Figure S2 in File S1 and Figure 8D, the ratios of ovary, ovotestis, and testis in *foxl2a*$^{-/-}$/*foxl2b*$^{-/-}$ mutants were very different, changing from seven ovaries:eight testes (~50%) at 35 dpf to 0 ovaries:15 testes (100% testes), and ~13–38% of ovotestes existed from 40 to 105 dpf. Moreover, we examined the gonadal histology of these sex reversal individuals from 35, 40, 50, and 60 dpf. As shown in Figure 8E, in comparison with normal ovaries with POs, PVOs, and VOs in heterozygous double mutant (*foxl2a*$^{-/-}$/*foxl2b*$^{+/-}$) females, the female individuals in homozygous *foxl2a*$^{-/-}$/*foxl2b*$^{-/-}$ mutants began to exhibit extensive oocyte degeneration and initiative sex reversal early from 40 dpf, even though they showed normal ovary differentiation at 35 dpf. At 35 dpf, numerous POs were destined for primitive ovaries, while apoptosis seemed to occur rapidly at 40 dpf, because there were many DPOs and cavities in the gonad tissues. Along with oocyte apoptosis and degeneration from 50 to 60 dpf, testicular tissues began to differentiate and numerously proliferated spermatogenic cells including SG, SPs, and spermatids filled the differentiated testes. After 60 dpf, it became increasingly difficult to identify female individuals, and only three individuals with secondary feminine characteristics and ovaries were discovered (Figure 8D and Figure S2 in File S1). At 150 dpf, all of the homozygous *foxl2a*$^{-/-}$/*foxl2b*$^{-/-}$ individuals examined had histologically normal testes (Figure 8D and Figure S2 in File S1), and were able to produce normal sperm and fertilize eggs. These data indicate that simultaneous disruption of *foxl2a* and *foxl2b* leads to

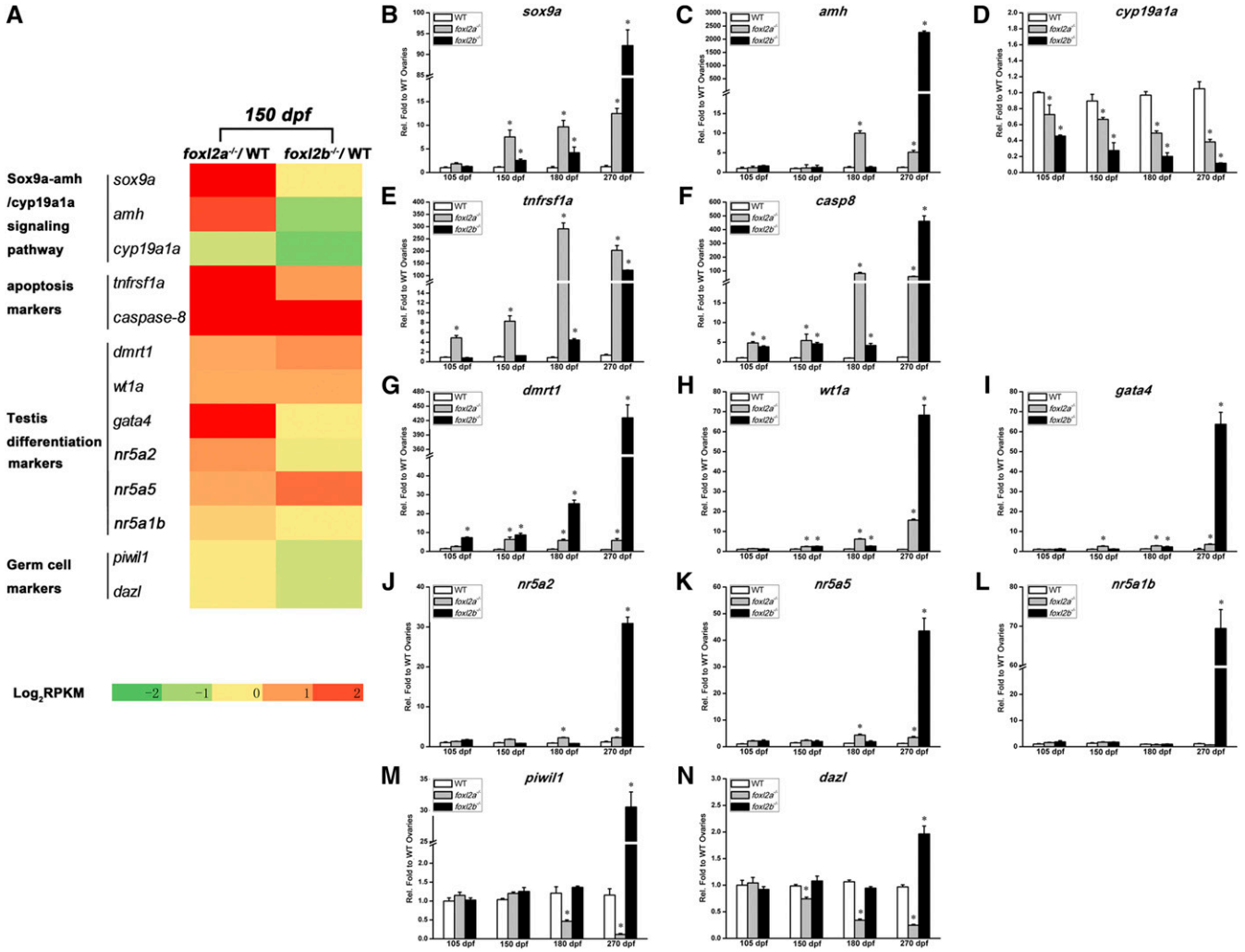

Figure 6 Transcriptome profiling changes of gonadal development-related genes in ovaries of *foxl2a*$^{-/-}$ and *foxl2b*$^{-/-}$ mutants. (A) Relatively transcribed changes of several kinds of gonadal development-related genes between *foxl2a*$^{-/-}$ and WT ovaries or *foxl2b*$^{-/-}$ and WT ovaries at 150 dpf. (B–N) Relative expression qRT-PCR detection of the indicated genes in WT, *foxl2a*$^{-/-}$, and *foxl2b*$^{-/-}$ ovaries from 105 to 270 dpf (n = 3). The qRT-PCR quantification of each gene expression is normalized to *actb1*, and the data are presented as mean ± SEM * $P \leq 0.05$ (Duncan's multiple range test).

complete sex reversal, and sex reversal occurs earlier in *foxl2a*$^{-/-}$/*foxl2b*$^{-/-}$ mutants than in *foxl2b*$^{-/-}$ mutants. Therefore, the roles of *foxl2a* and *foxl2b* might be compensatory in zebrafish ovary development and maintenance.

We also examined secondary sexual characteristics and testis development status of male *foxl2a*$^{-/-}$, *foxl2b*$^{-/-}$, and *foxl2a*$^{-/-}$/*foxl2b*$^{-/-}$ mutants at 35, 60, and 105 dpf. No significant abnormality in secondary sexual characteristics, testis differentiation and development, or spermatogenesis were observed in the males of three mutants. Similar to controls, some oocyte-like germ cells began to undergo apoptosis as demonstrated by dark-stained cytoplasm, and SCs containing SPs scattered in the gonadal tissues at 35 dpf. At 60 and 105 dpf, the male germ cells at all spermatogenic stages filled the lobules, and numerous free spermatozoa congregated into the lumen of all individuals of the three male mutants (Figure S7 in File S1). Furthermore, all male mutants were fertile because they all successfully spawned with females to produce normal offspring. Therefore, consistent with their sexually dimorphic expression, both *foxl2a* and *foxl2b* function specifically in the female gonad.

Zebrafish ovary differentiation and maintenance are cooperatively regulated by foxl2a and foxl2b

To test the molecular basis of the sex reversal that occurred in homozygous *foxl2a*$^{-/-}$/*foxl2b*$^{-/-}$ mutants, we examined the expression of gonad-related genes selected as above in the gonads from *foxl2a*$^{-/-}$/*foxl2b*$^{-/-}$ mutants at 60 dpf, which were classified into three stages: ovary, ovotestis, and testis. As expected, *sox9a*, *amh*, *dmrt1*, and other genes involved in the male development pathway all increased by several dozen- or even several 100-fold in ovotestis and testis compared to those in ovaries (Figure 9, A, B, and F–K); while ovary-related genes, such as *cyp19a1a* and *cyp11a1*, decreased significantly

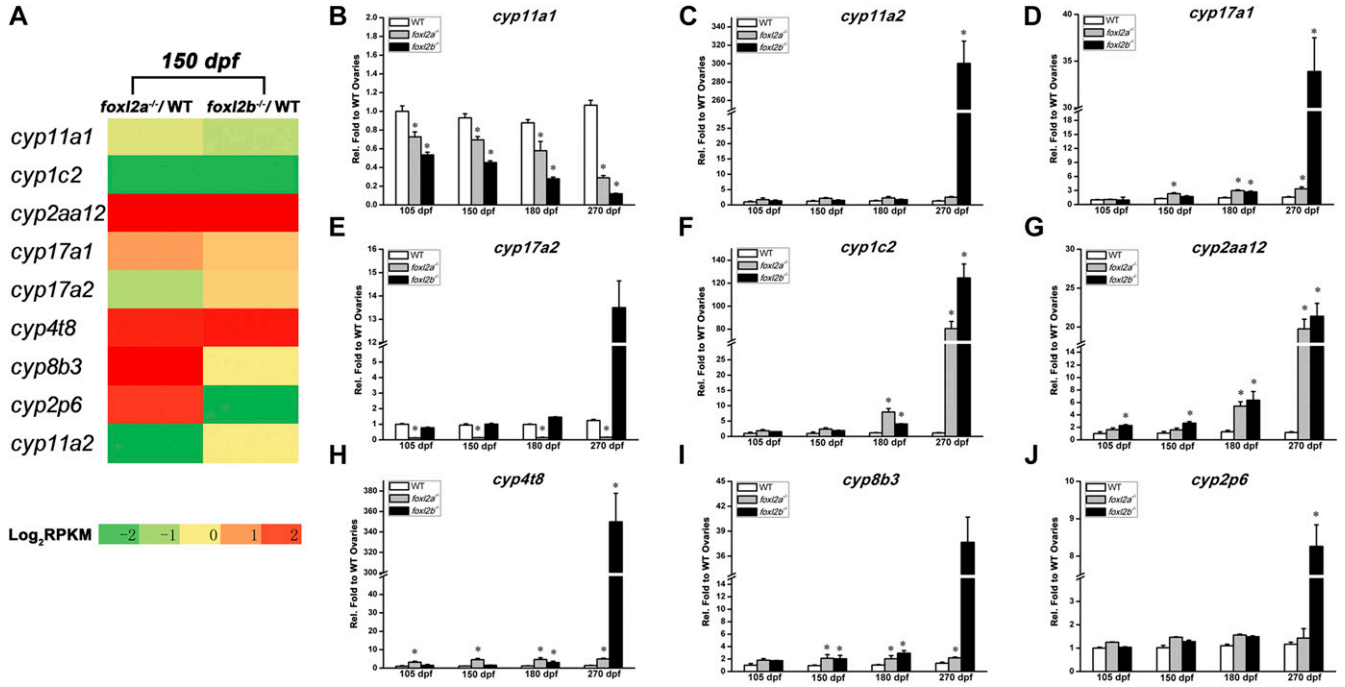

Figure 7 Transcriptome profiling changes of *cyp* genes in the ovaries of *foxl2a*$^{-/-}$ and *foxl2b*$^{-/-}$ mutants. (A) Relatively transcribed changes of nine *cyp* genes between *foxl2a*$^{-/-}$ and WT ovaries or *foxl2b*$^{-/-}$ and WT ovaries at 150 dpf. (B–J) Relative expression qRT-PCR detection of nine *cyp* genes in WT, *foxl2a*$^{-/-}$, and *foxl2b*$^{-/-}$ ovaries from 105 to 270 dpf ($n = 3$). The qRT-PCR quantification of each gene expression is normalized to *actb1*, and the data are presented as mean ± SEM * $P \leq 0.05$ (Duncan's multiple range test).

in ovotestis and were hardly detected in testis (Figure 9, C and N). Expression of all other *cyp* genes examined; as well as *tnfrsf1a*, *caspase-8*, *piwil1*, and *dazl* (Figure 9, D, E, L, and M); increased sharply in ovotestis and testis compared to those in ovaries (Figure 9, O–V). The altered expression levels in homozygous *foxl2a*$^{-/-}$/*foxl2b*$^{-/-}$ mutants were very similar to those of *foxl2b*$^{-/-}$ mutants at 270 dpf, implying that *foxl2a* deficiency enhances sex reversal caused by *foxl2b* knockout, whereas single *foxl2a* mutation results in different defects.

To test whether the functions of *foxl2a* and *foxl2b* are compensative in ovary development and maintenance, we assessed the expression changes of *foxl2a* in *foxl2b*$^{-/-}$ mutants and vice versa. Interestingly, the mRNA expression levels of both *foxl2a-1* and *foxl2a-2* were upregulated in the gonads of *foxl2b*$^{-/-}$ mutants before 180 dpf (Figure 9, W and X), and the reverse was also true (Figure 9Y). It seems that *foxl2a* and *foxl2b* can increase in expression to compensate for reduced expression at the other locus, eventually causing normal ovary development in both mutant backgrounds. However, *foxl2a* and *foxl2b* transcripts started to decrease in abundance from 180 dpf, when the mutants underwent POF or sex reversal. The pathological changes in the ovary might reduce or destroy the pathways involved in female gonad maintenance. This also suggests that the compensation between *foxl2a* and *foxl2b* in this process is partly divergent, causing the different phenotypes in two single mutants. Taken together, these results indicate that *foxl2a* and *foxl2b* cooperatively regulate zebrafish ovary differentiation and maintenance, whereas *foxl2b* plays more specific roles in maintaining female identity and preventing male transformation.

Discussion

Although SD and differentiation have been well studied in mammals and several sex-determining genes have been identified from different teleost species, this process is still a complicated affair in zebrafish (Liew and Orban 2013; Nagabhushana and Mishra 2016). Here we have revealed a sequential and divergent expression pattern between two zebrafish *foxl2* homologs, *foxl2a* and *foxl2b*, during oogenesis. Via histological and transcriptomic analyses of the *foxl2a*$^{-/-}$ and *foxl2b*$^{-/-}$ mutants, we propose a hypothesized model in which *foxl2a* and *foxl2b* cooperatively regulate zebrafish ovary differentiation and maintenance. As shown in Figure 10, unlike normal testis development, ovary development and oogenesis are significantly affected by loss of *foxl2a*, *foxl2b*, or both genes. Germ cell marker loci *piwil1* and *dazl* are sharply downregulated and the *sox9a-amh/cyp19a1a* signaling pathway and *foxl2b* are upregulated, which thereby results in POF in female *foxl2a*$^{-/-}$ mutants. In contrast to expression changes in *foxl2a*$^{-/-}$ premature ovaries, some testis differentiation and androgen-producing genes, such as *dmrt1*, *sox9*, *amh*, *wt1a*, *gata4*, *nr5a2*, *nr5a5*, *nr5a1b*, *cyp17a*, and *cyp11a2* are upregulated in female *foxl2b*$^{-/-}$ mutants and trigger partial sex reversal, although *foxl2a* expression increases. In homozygous

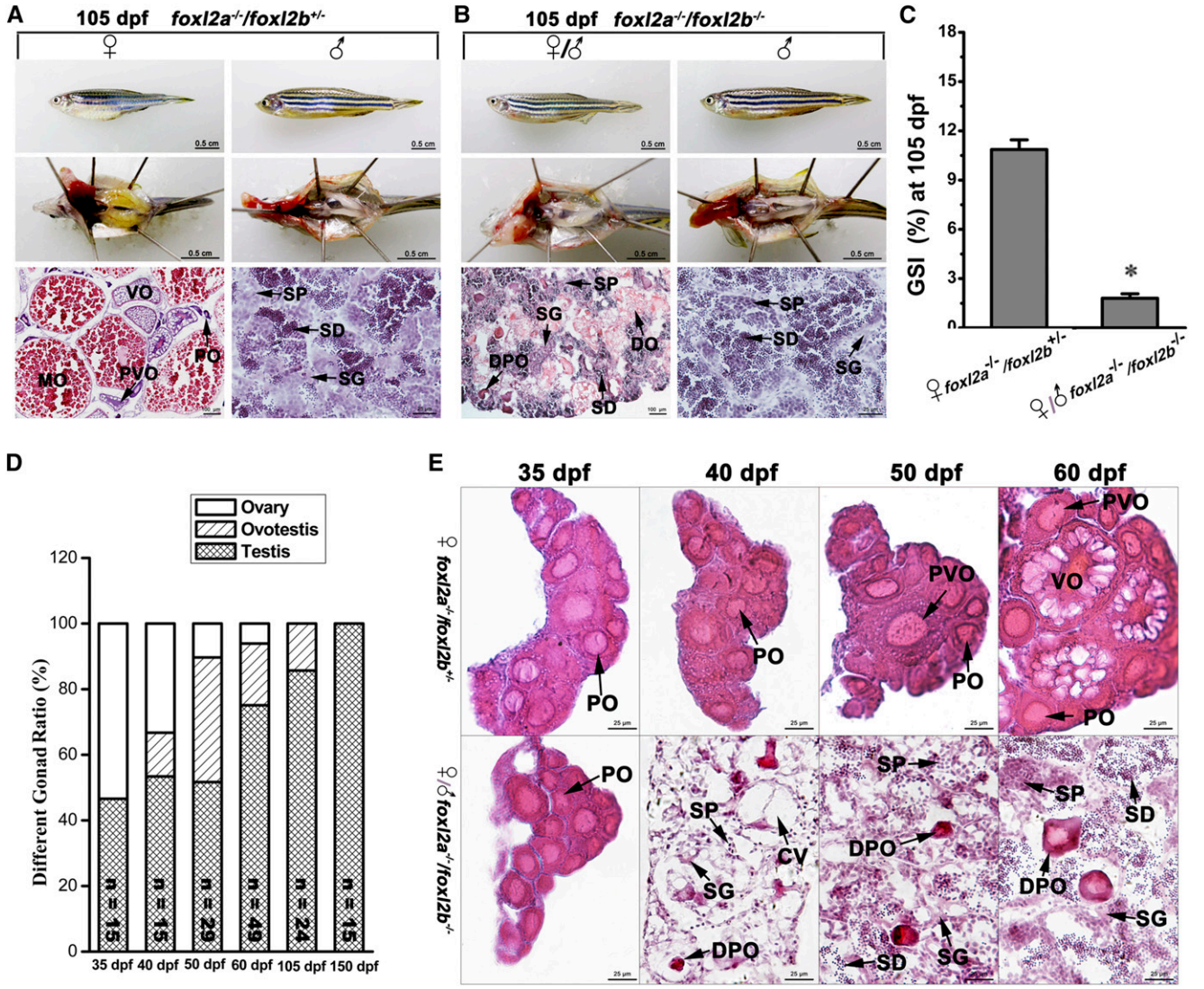

Figure 8 Complete sex reversal in homozygous *foxl2a*$^{-/-}$/*foxl2b*$^{-/-}$ females. (A and B) Gross morphology, anatomical, and gonadal histology examination of (A) heterozygous double mutants (*foxl2a*$^{-/-}$/*foxl2b*$^{+/-}$) (n = 13) and (B) homozygous double mutants (*foxl2a*$^{-/-}$/*foxl2b*$^{-/-}$) (n = 3) at 105 dpf. (C) GSI in *foxl2a*$^{-/-}$/*foxl2b*$^{+/-}$ and *foxl2a*$^{-/-}$/*foxl2b*$^{-/-}$ mutants at 105 dpf. Data are presented as mean ± SEM * $P \leq 0.05$ (Duncan's multiple range test). (D) Gonadal development status of homozygous *foxl2a*$^{-/-}$/*foxl2b*$^{-/-}$ individuals from young fishes to adults at 35, 40, 50, 60, 105, and 150 dpf. (E) Gonadal histology examination of heterozygous double mutants (*foxl2a*$^{-/-}$/*foxl2b*$^{+/-}$) and homozygous double mutants (*foxl2a*$^{-/-}$/*foxl2b*$^{-/-}$) at 35 dpf (n = 7), 40 dpf (n = 3), 50 dpf (n = 7), and 60 dpf (n = 9). ♀, females; ♂, males; CV, cavity; SD, spermatid. Bars are shown at bottom right of the images.

foxl2a$^{-/-}$/*foxl2b*$^{-/-}$ females, a complete sex reversal occurs early, and numerous genes in the testis development pathway are sharply activated to lead to complete sex reversal and formation of ovotestis and testis.

Consistent with other teleosts (Caulier *et al.* 2015), zebrafish *foxl2a1/2* and *foxl2b* all showed sexual dimorphism. Zebrafish *foxl2a* transcripts are mainly expressed in the ovary at 35 dpf and decline while maturation proceeds. In mice, *Foxl2* is expressed initially at 12.5 days postconception, and occurs in the granulosa cells of early follicles but gradually reduces as oocytes proceed to maturation (Schmidt 2004; Nakamoto *et al.* 2006). *Foxl2* is also highly expressed in Nile tilapia *XX* gonads as early as 5 days after hatching (dah), increases linearly until 35 dah, and remains high at 70 dah (Ijiri *et al.* 2008). However, *foxl2b* increases from immature stages and peaks at the mature and spawning stage (Figure 10), similar to *Foxl2* in chicken (Govoroun *et al.* 2004), Korean rockfish (Mu *et al.* 2013), and African sharptooth catfish (Sridevi and Senthilkumaran 2011). The sequential and divergent expression patterns of zebrafish *foxl2a* and *foxl2b* during oogenesis (Figure 10) indicate that *foxl2a* and *foxl2b* may have undergone subfunctionalization after their divergence.

The role of *Foxl2* is complicated because of the disparate effects in humans and other mammals, such as mouse and goat (Ottolenghi *et al.* 2007). Its functions in development

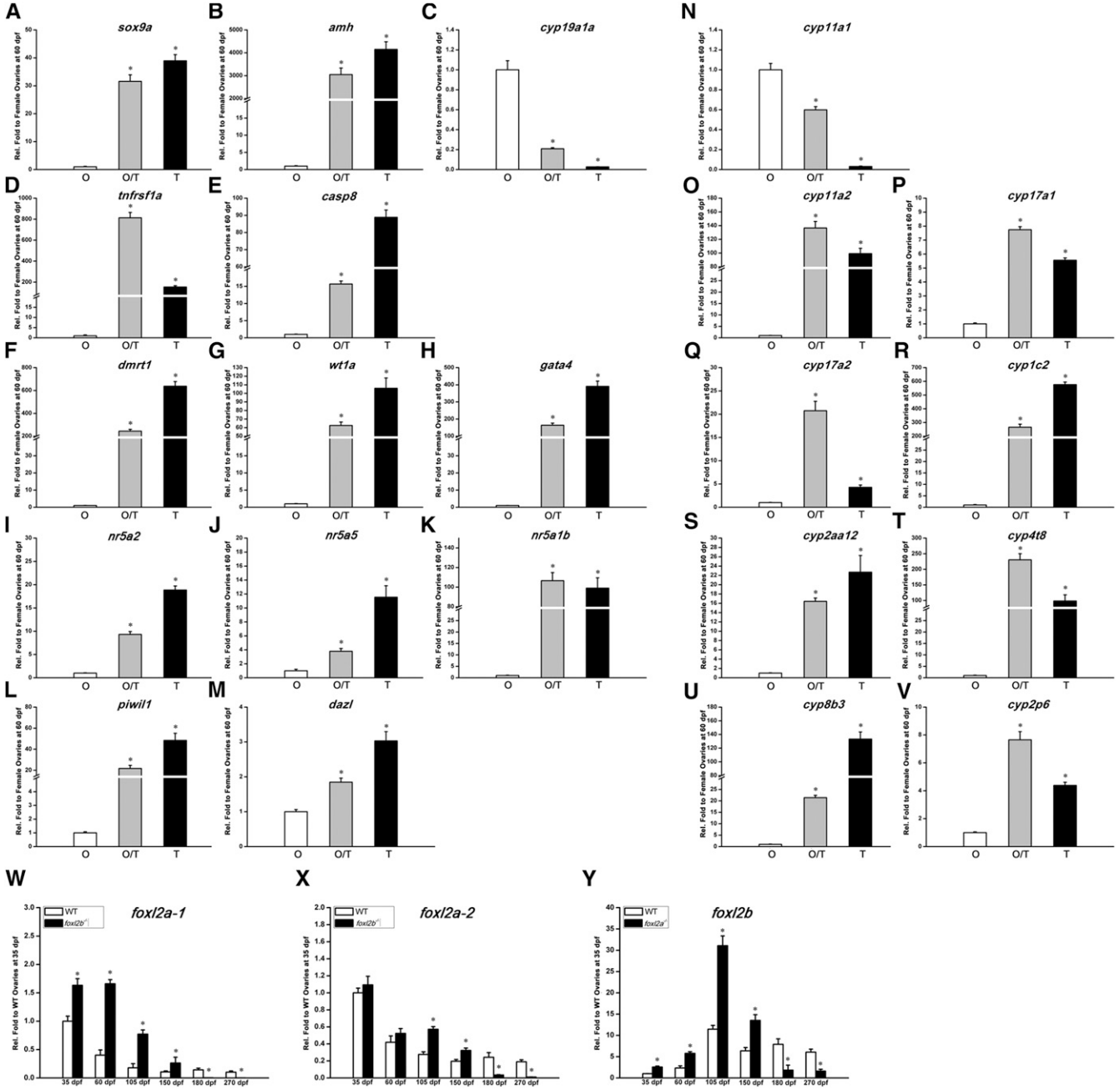

Figure 9 *Foxl2a* and *foxl2b* cooperatively regulate ovary differentiation and maintenance in zebrafish. (A–V) Relative expression qRT-PCR detection of the indicated genes in ovary (O), ovotestis (O/T), and testis (T) of homozygous double mutants (*foxl2a*$^{-/-}$/*foxl2b*$^{-/-}$) at 60 dpf (n = 3). Gene names are indicated at the top. (W–Y) Relative expression qRT-PCR detection of (W) *foxl2a-1*, (X) *foxl2a-2*, and (Y) *foxl2b* in the ovaries of WT and *foxl2b* mutants (*foxl2b*$^{-/-}$) or *foxl2a* mutants (*foxl2a*$^{-/-}$) from 35 to 270 dpf, respectively (n = 3). The qRT-PCR quantification of each gene expression is normalized to *actb1*, and the data are presented as mean ± SEM * $P \leq 0.05$ (Duncan's multiple range test).

were first suggested by studying BPES, which is characterized by eyelid/forehead anomalies associated with POF, an early loss of normal ovarian function (Crisponi *et al.* 2001; De Baere *et al.* 2003; Meduri *et al.* 2010). *Foxl2*$^{-/-}$ mice showed craniofacial and eyelid defects, a complete failure of follicle formation, and partial sex reversal in females (Schmidt 2004; Uda *et al.* 2004; Ottolenghi 2005; Ottolenghi *et al.* 2007). Conditional loss of *Foxl2* in the adult ovary resulted in autonomous reprogramming of oocyte-supporting granulosa cells into testis-specific Sertoli-like cells (Uhlenhaut *et al.* 2009). In goats, *FOXL2* mutation led to the polled intersex syndrome, which associated polledness and *XX* female-to-male sex reversal in a recessive manner (Pailhoux *et al.* 2001). In our study, zebrafish homozygous *foxl2a*$^{-/-}$ F_3 females showed normal ovarian differentiation and growth at the onset of sexual maturity, but ~60% of *foxl2a*$^{-/-}$ females

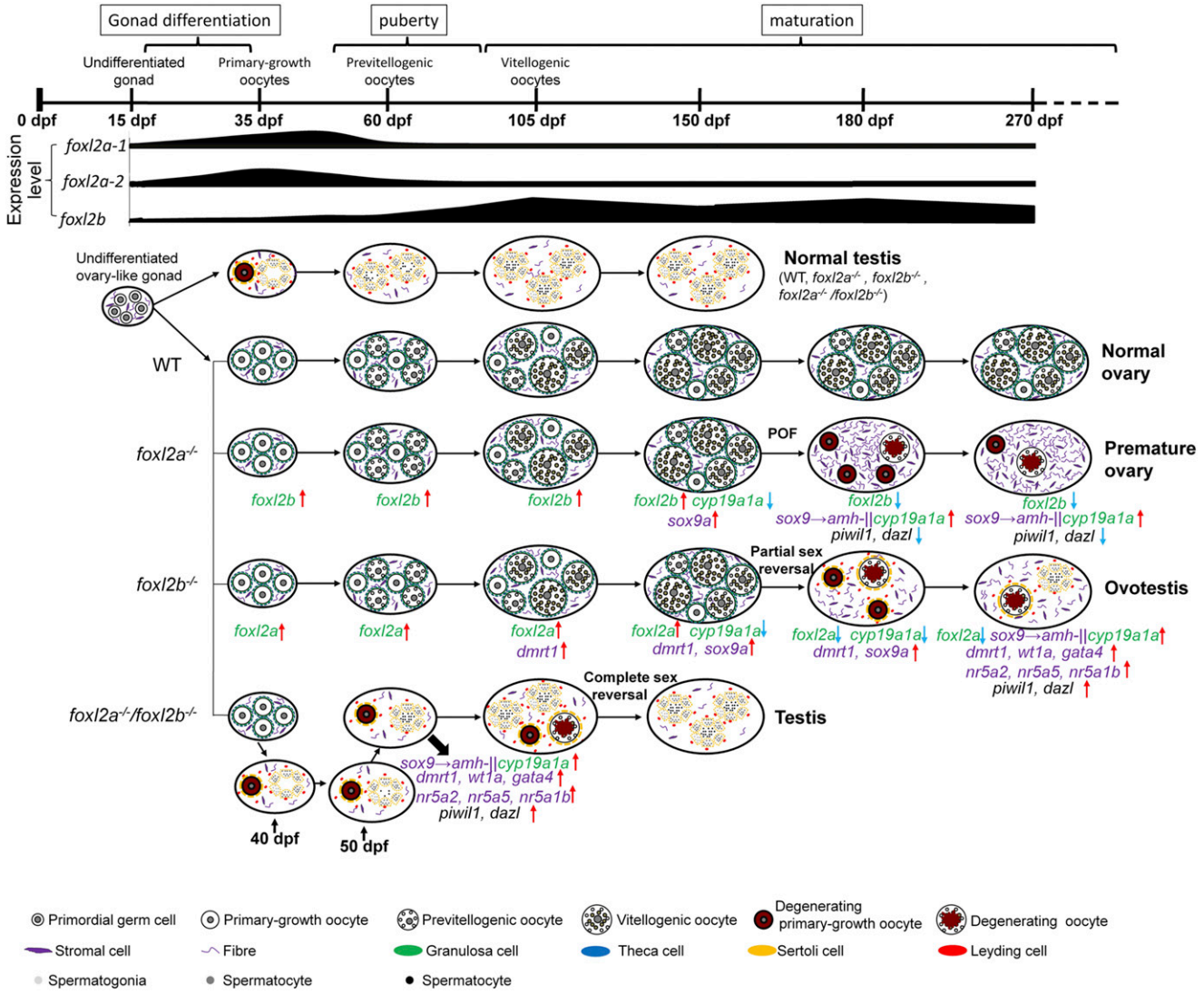

Figure 10 A hypothesized diagram for cooperative regulation between *foxl2a* and *foxl2b* in ovary development and maintenance of zebrafish. Different gonad development stages; expression level changes of *foxl2a-1*, *foxl2a-2*, and *foxl2b*; different status gonads including normal testis, normal ovary, premature ovary, and ovotestis; different germ cells and gonad-related somatic cells; different gonadal development-related genes; and their upregulation and downregulation expression are indicated in detail. Red ↑, upregulation; blue ↓, downregulation.

exhibited ovarian histological changes at 270 dpf, with the degeneration of ovarian tissue, presence of atretic follicles, reduction of germ cells, and proliferation of somatic cells (Figure 4 and Figure S2 in File S1), similar to the ovarian senescence that occurred in the 18-month-old female zebrafish (Turola *et al.* 2015). However, no WT zebrafish exhibited ovarian senescence before 270 dpf, indicating that ovarian senescence was promoted in the *foxl2a*$^{-/-}$ mutants. The accelerated ovarian aging phenotype in *foxl2a*$^{-/-}$ mutants is reminiscent of human BPES. Meanwhile, disruption of zebrafish *foxl2b* led to partial sex reversal from female to male after spawning a few times (Figure 5), similar to the case in mouse and goat. Furthermore, the expression of genes related to gonad development was also different in *foxl2a*$^{-/-}$ and *foxl2b*$^{-/-}$ mutants (Figure 6, Figure 7, and Table S4). Therefore, zebrafish *foxl2a* and *foxl2b* have evolved functional divergence. On the other hand, the complete sex reversal (Figure 8) and robust increasing expression of testicular differentiation genes occurred earlier (Figure 9) in *foxl2a*$^{-/-}$/*foxl2b*$^{-/-}$ double female mutants than those in any single mutants, suggesting the compensation and redundancy between *foxl2a* and *foxl2b*. Indeed, the compensation to a deficiency in either gene was not only observed in the transcriptome profiling comparisons (Table S4), but also confirmed by qRT-PCR (Figure 9, W–Y). Taken together, *foxl2a* and *foxl2b* work differentially and cooperate to manipulate zebrafish ovary differentiation and maintenance.

Foxl2 and Sox9, as the yin and yang of sex maintenance, antagonize each other's actions in the establishment and maintenance of granulosa cells and Sertoli cells (Uhlenhaut *et al.* 2009). In this case, a significant increase of *sox9a* transcript takes place both in *foxl2a*$^{-/-}$ and *foxl2b*$^{-/-}$ mutated

ovaries at 150 dpf (Figure 6, A and B, and Table S4), although no apparent abnormalities of ovarian morphology and histology were observed (Figure 4B). The upregulation of *sox9a* in *foxl2a*$^{-/-}$ and *foxl2b*$^{-/-}$ mutated ovaries suggests that zebrafish *sox9a* transcription might be directly repressed by Foxl2s in the ovary, similar to mouse. A *cis*-regulatory element for testis-specific *Sox9* expression (TESCO) has been identified in mouse *Sox9* (Sekido and Lovell-Badge 2008) and proven to be negatively modulated by FOXL2 (Uhlenhaut *et al.* 2009). However, the well-conserved 1.4-kb TESCO sequence was only found in placental mammals, not in chicken, Fugu, or zebrafish (Sekido and Lovell-Badge 2008). Further analyses revealed that a 180-bp evolutionarily conserved region (ECR) within the SOX9 testis enhancer containing the conserved FHD binding site was identified in chicken, lizard, and frog, but not in fish (Bagheri-Fam *et al.* 2010). After searching the zebrafish draft genome by using frog ECR as the query, a 180-bp sequence showing a 43% identity to frog ECR was found in the 68.1 kb upstream of the zebrafish *sox9a* gene, where seven conserved FHD binding sites occured. This suggests that zebrafish Foxl2s might also inhibit the testis-differentiation program, mainly through repressing *sox9a* as occurs in mouse (Uhlenhaut *et al.* 2009). Interestingly, *sox9a* expression changes corresponding to the disruption of *foxl2a* and *foxl2b* are not the same (Figure 6B), implying that a subtle differential regulatory mechanism remains for further investigation in zebrafish. During mammalian male fetal sex differentiation, *Sox9* activates the expression of *Amh* (de Santa Barbara *et al.* 1998), which induces the degeneration of Müllerian ducts (Behringer *et al.* 1994) and inhibits *Cyp19a1* expression (Rouiller-Fabre *et al.* 1998). Along with the upregulation of *sox9a*, *amh* increased in expression while *cyp19a1a* decreased in abundance in all three zebrafish mutant ovaries (Figure 6, B–D, and Figure 9, A–C), implying that a *sox9a-amh/cyp19a1a* pathway *should* be highly conserved in vertebrates.

Dmrt1 is a central regulator in vertebrate testis determination and differentiation (Xia *et al.* 2007; Matson and Zarkower 2012; Li *et al.* 2014). It is required for mammalian postnatal testis differentiation (Raymond *et al.* 2000), and its homologous genes were identified as SD genes in chicken (Smith *et al.* 2009), *X. laevis* (Yoshimoto *et al.* 2008), and medaka (Matsuda *et al.* 2002). In conditional *Foxl2* deletion mice ovotestis, *Dmrt1* is one of the most upregulated genes, indicating that FOXL2 may directly repress *Dmrt1* transcription (Uhlenhaut *et al.* 2009). Interestingly, *sox9a* and *dmrt1* exhibited differentially dynamic expression patterns between *foxl2a*$^{-/-}$/WT and *foxl2b*$^{-/-}$/WT ovaries (Figure 6, B and G). In accordance with no sex reversal individuals observed in *foxl2a*$^{-/-}$ mutants, *dmrt1* only slightly increased in expression at 270 dpf. However, *dmrt1* and other testicular differentiation genes, such as *sox9a* (Chiang *et al.* 2001), *amh* (Schulz *et al.* 2001), *wt1a* (Hammes *et al.* 2001), *gata4* (Tevosian *et al.* 2002), *nr5a2*, *nr5a5*, and *nr5a1b* (Luo *et al.* 1994; Von Hofsten *et al.* 2005a,b), were all robustly upregulated in ovotestis of *foxl2b*$^{-/-}$ mutants along with sex reversal (Figure 6, B, C, and G–L), which indicated that *foxl2b* might play a more dominant role in suppressing testis-differentiation signaling than *foxl2a*. Although many key players, such as *foxl2a*, *sox9*, *amh*, *dmrt1*, and *cyp19a1*, show sexually dimorphic expression in zebrafish, the interactions within the proposed transcriptional network are unclear. The establishments of the *foxl2a*$^{-/-}$, *foxl2b*$^{-/-}$, and *foxl2a*$^{-/-}$/*foxl2b*$^{-/-}$ mutants in this study will provide a model to definitively clarify the regulatory interactions among these factors.

The CYP enzymes catalyze oxidation reactions and have diverse functions in vertebrates. It is well known that some *cyp* family members play essential roles in steroidogenesis, including estrogen production (Stoilov 2001; Payne and Hales 2004; Chang *et al.* 2005; Baldwin *et al.* 2009; Huang *et al.* 2009; Heule *et al.* 2014). Many studies have been done to reveal the relevance of *foxl2*, aromatase, and sex hormones in the teleost brain-pituitary-gonad axis, in which *foxl2* was found to regulate estrogen synthesis via transcriptional regulation of *cyp19* (Baron 2004; Wang *et al.* 2007; Navarro-Martín *et al.* 2011; Sridevi *et al.* 2012; Crespo *et al.* 2013), and in turn, the ovarian *foxl2* was upregulated by estrogen treatment (Baron 2004; Liu *et al.* 2007; Wu *et al.* 2008; Jiang *et al.* 2011; Wang *et al.* 2012). Zebrafish have a total of 94 *cyp* genes (Goldstone *et al.* 2010), in which 59 *cyp* genes were identified from transcriptome files (Table S4) and 9 *cyp* genes showing dynamic expression changes in three mutants were confirmed by qRT-PCR (Figure 7 and Figure 9). The differential effects of *foxl2a* and *foxl2b* on gonadal steroidogenesis need further investigation to determine the regulatory mechanisms between *foxl2s* and *cyps*.

Zebrafish male development undergoes a transformation of juvenile ovary to testis in adolescence (Uchida *et al.* 2002; Maack and Segner 2003). During this process, the *sox9a-amh/cyp19a1a* pathway linked to MAPK-p53 signaling precedes oocyte apoptosis and degeneration, and the expression of *sox9a* increased in the transforming gonads activates stromal cells and increases extracellular matrix (ECM) production (Sun *et al.* 2013). Similarly, we observed the DOs surrounded by gonadal matrix and a massive increase of somatic cells in the three mutants (Figure 4, Figure 5, and Figure 8). The comparative transcriptome analyses revealed that the TNF signaling pathway, cytokine-cytokine receptor interaction, and "ECM-receptor interaction" pathways were enriched in both *foxl2a*$^{-/-}$/WT and *foxl2b*$^{-/-}$/WT ovaries (Table S5). Meanwhile, the DOs were dissociated from adjacent cells with a marked vacuolation in the three female mutants (Figure 4, Figure 5, and Figure 8), implying that the oocytes and follicle cells lost their tight junctions with adjacent cells. Consistent with these changes, the top 30 pathways in both *foxl2a*$^{-/-}$/WT and *foxl2b*$^{-/-}$/WT ovaries include several pathways involved in cell adhesion, such as cell adhesion molecules, focal adhesion, gap junction, and regulation of actin cytoskeleton (Table S5).

In conclusion, this study established *foxl2a* knockout, *foxl2b* knockout, and double knockout zebrafish and revealed POF, partial sex reversal, and complete sex reversal in the three mutants, respectively. Based on the comparative transcriptome analyses and dynamic expression patterns of DEGs, we propose that *foxl2a* and *foxl2b* cooperate with each other to regulate zebrafish ovary differentiation and maintenance, and that *foxl2b* plays a dominant role in preventing the ovary from differentiating as testis. In addition, these *foxl2*-related mutants also provide some model systems to study human POF and the mechanism determining fish sex.

Acknowledgments

We are grateful to Wenhua Li and Chenyan Mou for helping to construct the transcription activator-like effector nucleases (TALEN) plasmids and to screen the mutants. This work was supported by the Strategic Priority Research Program of the Chinese Academy of Sciences (XDA08030201); the Autonomous Project of the State Key Laboratory of Freshwater Ecology and Biotechnology (2016FBZ01); and the Autonomous Project of the Institute of Hydrobiology, Chinese Academy of Sciences (Y25A171).

Literature Cited

Alam, M. A., Y. Kobayashi, R. Horiguchi, T. Hirai, and M. Nakamura, 2008 Molecular cloning and quantitative expression of sexually dimorphic markers Dmrt1 and Foxl2 during female-to-male sex change in *Epinephelus merra*. Gen. Comp. Endocrinol. 157: 75–85.

Anderson, J. L., A. R. Mari, I. Braasch, A. Amores, P. Hohenlohe *et al.*, 2012 Multiple sex-associated regions and a putative sex chromosome in zebrafish revealed by RAD mapping and population genomics. PLoS One 7: e40701.

Bachtrog, D., J. E. Mank, C. L. Peichel, M. Kirkpatrick, S. P. Otto *et al.*, 2014 Sex determination: why so many ways of doing it? PLoS Biol. 12: e1001899.

Bagheri-Fam, S., A. H. Sinclair, P. Koopman, and V. R. Harley, 2010 Conserved regulatory modules in the Sox9 testis-specific enhancer predict roles for SOX, TCF/LEF, Forkhead, DMRT, and GATA proteins in vertebrate sex determination. Int. J. Biochem. Cell Biol. 42: 472–477.

Baldwin, W. S., P. B. Marko, and D. R. Nelson, 2009 The cytochrome P450 (CYP) gene superfamily in Daphnia pulex. BMC Genomics 10: 169.

Baroiller, J. F., H. D'Cotta, and E. Saillant, 2009 Environmental effects on fish sex determination and differentiation. Sex Dev. 3: 118–135.

Baron, D., 2004 An evolutionary and functional analysis of FoxL2 in rainbow trout gonad differentiation. J. Mol. Endocrinol. 33: 705–715.

Barske, L. A., and B. Capel, 2008 Blurring the edges in vertebrate sex determination. Curr. Opin. Genet. Dev. 18: 499–505.

Behringer, R. R., M. J. Finegold, and R. L. Cate, 1994 Müllerian-inhibiting substance function during mammalian sexual development. Cell 79: 415–425.

Bell, G., 1982 *The Masterpiece of Nature: the Evolution of Genetics of Sexuality*. University of California Press, Berkeley, CA.

Benayoun, B. A., S. Caburet, and R. A. Veitia, 2011 Forkhead transcription factors: key players in health and disease. Trends Genet. 27: 224–232.

Bhat, I. A., M. A. Rather, J. Y. Dar, and R. Sharma, 2016 Molecular cloning, computational analysis and expression pattern of forkhead box l2 (Foxl2) gene in catfish. Comput. Biol. Chem. 64: 9–18.

Bonduriansky, R., 2009 Reappraising sexual coevolution and the sex roles. PLoS Biol. 7: e1000255.

Bustin, S. A., V. Benes, J. A. Garson, J. Hellemans, J. Huggett *et al.*, 2009 The miqe guidelines: minimum information for publication of quantitative real-time PCR experiments. Clin. Chem. 55: 611–622.

Carlsson, P., and M. Mahlapuu, 2002 Forkhead transcription factors: key players in development and metabolism. Dev. Biol. 250: 1–23.

Caulier, M., F. Brion, E. Chadili, C. Turies, B. Piccini *et al.*, 2015 Localization of steroidogenic enzymes and Foxl2a in the gonads of mature zebrafish (*Danio rerio*). Comp. Biochem. Physiol. A Mol. Integr. Physiol. 188: 96–106.

Chang, K. T., L. Sefc, O. Psenak, M. Vokurka, and E. Necas, 2005 Early fetal liver readily repopulates B lymphopoiesis in adult bone marrow. Stem Cells 23: 230–239.

Chiang, E. F. L., C. I. Pai, M. Wyatt, Y. L. Yan, J. Postlethwait *et al.*, 2001 Two sox9 genes on duplicated zebrafish chromosomes: expression of similar transcription activators in distinct sites. Dev. Biol. 231: 149–163.

Cocquet, J., E. Pailhoux, F. Jaubert, N. Servel, X. Xia *et al.*, 2002 Evolution and expression of FOXL2. J. Med. Genet. 39: 916–921.

Crespo, B., O. Lan-Chow-Wing, A. Rocha, S. Zanuy, and A. Gómez, 2013 Foxl2 and foxl3 are two ancient paralogs that remain fully functional in teleosts. Gen. Comp. Endocrinol. 194: 81–93.

Crisponi, L., M. Deiana, A. Loi, F. Chiappe, M. Uda *et al.*, 2001 The putative forkhead transcription factor FOXL2 is mutated in blepharophimosis/ptosis/epicanthus inversus syndrome. Nat. Genet. 27: 159–166.

De Baere, E., D. Beysen, C. Oley, B. Lorenz, J. Cocquet *et al.*, 2003 FOXL2 and BPES: mutational hotspots, phenotypic variability, and revision of the genotype-phenotype correlation. Am. J. Hum. Genet. 72: 478–487.

de Santa Barbara, P., B. Moniot, F. Poulat, B. Boizet, and P. Berta, 1998 Steroidogenic factor-1 regulates transcription of the human anti-mullerian hormone receptor. J. Biol. Chem. 273: 29654–29660.

Desjardins, J. K., and R. D. Fernald, 2009 Fish sex: why so diverse? Curr. Opin. Neurobiol. 19: 648–653.

Devlin, R. H., and Y. Nagahama, 2002 Sex determination and sex differentiation in fish: an overview of genetic, physiological, and environmental influences. Aquaculture 208: 191–364.

Fetterman, C. D., B. Rannala, and M. A. Walter, 2008 Identification and analysis of evolutionary selection pressures acting at the molecular level in five forkhead subfamilies. BMC Evol. Biol. 8: 261.

Goldstone, J. V., A. G. McArthur, A. Kubota, J. Zanette, T. Parente *et al.*, 2010 Identification and developmental expression of the full complement of cytochrome P450 genes in Zebrafish. BMC Genomics 11: 643.

Govoroun, M. S., M. Pannetier, E. Pailhoux, J. Cocquet, J. P. Brillard *et al.*, 2004 Isolation of chicken homolog of the FOXL2 gene and comparison of its expression patterns with those of aromatase during ovarian development. Dev. Dyn. 231: 859–870.

Grunwald, D. J., and J. S. Eisen, 2002 Headwaters of the zebrafish emergence of a new model vertebrate. Nat. Rev. Genet. 3: 717–724.

Gui, J. F., and Z. Y. Zhu, 2012 Molecular basis and genetic improvement of economically important traits in aquaculture animals. Sci Bull. 57: 1751–1760.

Hammes, A., J. K. Guo, G. Lutsch, J. R. Leheste, D. Landrock *et al.*, 2001 Two splice variants of the Wilms' tumor 1 gene have

distinct functions during sex determination and nephron formation. Cell 106: 319–329.
Hannenhalli, S., and K. H. Kaestner, 2009 The evolution of Fox genes and their role in development and disease. Nat. Rev. Genet. 10: 233–240.
Hattori, R. S., Y. Murai, M. Oura, S. Masuda, S. K. Majhi *et al.*, 2012 A Y-linked anti-Mullerian hormone duplication akes over a critical role in sex determination. Proc. Natl. Acad. Sci. USA 109: 2955–2959.
Heule, C., W. Salzburger, and A. Bohne, 2014 Genetics of sexual development: an evolutionary playground for fish. Genetics 196: 579–591.
Howe, K., M. D. Clark, C. F. Torroja, J. Torrance, C. Berthelot *et al.*, 2013 The zebrafish reference genome sequence and its relationship to the human genome. Nature 496: 498–503.
Huang, P., A. Xiao, X. Tong, Y. Zu, Z. Wang *et al.*, 2014 TALEN construction via "Unit Assembly" method and targeted genome modifications in zebrafish. Methods 69: 67–75.
Huang, W., L. Zhou, Z. Li, and J. F. Gui, 2009 Expression pattern, cellular localization and promoter activity analysis of ovarian aromatase (Cyp19a1a) in protogynous hermaphrodite red-spotted grouper. Mol. Cell. Endocrinol. 307: 224–236.
Ijiri, S., H. Kaneko, T. Kobayashi, D. S. Wang, F. Sakai *et al.*, 2008 Sexual dimorphic expression of genes in gonads during early differentiation of a teleost fish, the Nile tilapia *Oreochromis niloticus*. Biol. Reprod. 78: 333–341.
Jiang, W., Y. Yang, D. Zhao, X. Liu, J. Duan *et al.*, 2011 Effects of sexual steroids on the expression of foxl2 in *Gobiocypris rarus*. Comp. Biochem. Physiol. B Biochem. Mol. Biol. 160: 187–193.
Jorgensen, A., J. E. Morthorst, O. Andersen, L. J. Rasmussen, and P. Bjerregaard, 2008 Expression profiles for six zebrafish genes during gonadal sex differentiation. Reprod. Biol. Endocrinol. 6: 25.
Kaestner, K. H., W. Knochel, and D. E. Martinez, 2000 Unified nomenclature for the winged helix/forkhead transcription factors. Genes Dev. 14: 142–146.
Kamiya, T., W. Kai, S. Tasumi, A. Oka, T. Matsunaga *et al.*, 2012 A trans-species missense SNP in Amhr2 is associated with sex determination in the tiger pufferfish, *Takifugu rubripes* (fugu). PLoS Genet. 8: e1002798.
Kobayashi, Y., R. Horiguchi, R. Nozu, and M. Nakamura, 2010 Expression and localization of forkhead transcriptional factor 2 (Foxl2) in the gonads of protogynous wrasse, *Halichoeres trimaculatus*. Biol. Sex Differ. 1: 3.
Kocer, A., I. Pinheiro, M. Pannetier, L. Renault, P. Parma *et al.*, 2008 R-spondin1 and FOXL2 act into two distinct cellular types during goat ovarian differentiation. BMC Dev. Biol. 8: 36.
Li, B., and C. N. Dewey, 2011 RSEM: accurate transcript quantification from RNA-Seq data with or without a reference genome. BMC Bioinformatics 12: 93–99.
Li, M. H., H. H. Yang, M. R. Li, Y. L. Sun, X. L. Jiang *et al.*, 2013 Antagonistic roles of Dmrt1 and Foxl2 in sex differentiation via estrogen production in tilapia as demonstrated by TALENs. Endocrinology 154: 4814–4825.
Li, X. Y., Z. Li, X. J. Zhang, L. Zhou, and J. F. Gui, 2014 Expression characterization of testicular DMRT1 in both Sertoli cells and spermatogenic cells of polyploid gibel carp. Gene 548: 119–125.
Li, X. Y., Q. Y. Zhang, J. Zhang, L. Zhou, Z. Li *et al.*, 2016 Extra microchromosomes play male determination role in polyploid gibel carp. Genetics 203: 1415–1424.
Liew, W. C., and L. Orban, 2013 Zebrafish sex: a complicated affair. Brief. Funct. Genomics 13: 172–187.
Liu, Z., F. Wu, B. Jiao, X. Zhang, C. Hu *et al.*, 2007 Molecular cloning of doublesex and mab-3-related transcription factor 1, forkhead transcription factor gene 2, and two types of cytochrome P450 aromatase in Southern catfish and their possible roles in sex differentiation. J. Endocrinol. 194: 223–241.
Livak, K. J., and T. D. Schmittgen, 2001 Analysis of relative gene expression data using real-time quantitative PCR and the 2(-Delta Delta C(T)) method. Methods 25: 402–408.
Loffler, K. A., D. Zarkower, and P. Koopman, 2003 Etiology of ovarian failure in blepharophimosis ptosis epicanthus inversus syndrome: FOXL2 is a conserved, early-acting gene in vertebrate ovarian development. Endocrinology 144: 3237–3243.
Luo, X. R., Y. Y. Ikeda, and K. L. Parker, 1994 A cell-specific nuclear receptor is essential for adrenal and gonadal development and sexual-differentiation. Cell 77: 481–490.
Maack, G., and H. Segner, 2003 Morphological development of the gonads in zebrafish. J. Fish Biol. 62: 895–906.
Marín, I., and B. S. Baker, 1998 The evolutionary dynamics of sex determination. Science 281: 1990–1994.
Matson, C. K., and D. Zarkower, 2012 Sex and the singular DM domain: insights into sexual regulation, evolution and plasticity. Nat. Rev. Genet. 13: 163–174.
Matsuda, M., Y. Nagahama, A. Shinomiya, T. Sato, C. Matsuda *et al.*, 2002 DMY is a Y-specific DM-domain gene required for male development in the medaka fish. Nature 417: 559–563.
Meduri, G., A. Bachelot, C. Duflos, B. Bstandig, C. Poirot *et al.*, 2010 FOXL2 mutations lead to different ovarian phenotypes in BPES patients: Case Report. Hum Reprod. 25: 235–243.
Meeker, N. D., S. A. Hutchinson, L. Ho, and N. S. Trecle, 2007 Method for isolation of PCR-ready genomic DNA from zebrafish tissues. Biotechniques 43: 610–614.
Mei, J., and J. F. Gui, 2015 Genetic basis and biotechnological manipulation of sexual dimorphism and sex determination in fish. Sci. China Life Sci. 58: 124–136.
Mu, W. J., H. S. Wen, J. F. Li, and F. He, 2013 Cloning and expression analysis of Foxl2 during the reproductive cycle in Korean rockfish, *Sebastes schlegeli*. Fish Physiol. Biochem. 39: 1419–1430.
Myosho, T., H. Otake, H. Masuyama, M. Matsuda, Y. Kuroki *et al.*, 2012 Tracing the emergence of a novel sex-determining gene in medaka, *Oryzias luzonensis*. Genetics 191: 163–170.
Nagabhushana, A., and R. K. Mishra, 2016 Finding clues to the riddle of sex determination in zebrafish. J. Biosci. 41: 145–155.
Nakamoto, M., M. Matsuda, D.-S. Wang, Y. Nagahama, and N. Shibata, 2006 Molecular cloning and analysis of gonadal expression of Foxl2 in the medaka, *Oryzias latipes*. Biochem. Biophys. Res. Commun. 344: 353–361.
Nakamoto, M., D. S. Wang, A. Suzuki, M. Matsuda, Y. Nagahama *et al.*, 2007 Dax1 suppresses P450arom expression in medaka ovarian follicles. Mol. Reprod. Dev. 74: 1239–1246.
Nakamura, M., T. Kobayashi, X. T. Chang, and Y. Nagahama, 1998 Gonadal sex differentiation in teleost fish. J. Exp. Zool. 281: 362–372.
Navarro-Martín, L., J. Viñas, L. Ribas, N. Díaz, A. Gutiérrez *et al.*, 2011 DNA methylation of the gonadal aromatase (cyp19a) promoter is involved in temperature-dependent sex ratio shifts in the European sea bass. PLoS Genet. 7: e1002447.
Nishimura, T., and M. Tanaka, 2014 Gonadal development in fish. Sex Dev. 8: 252–261.
Ota, S., Y. Hisano, M. Muraki, K. Hoshijima, T. J. Dahlem *et al.*, 2013 Efficient identification of TALEN-mediated genome modifications using heteroduplex mobility assays. Genes Cells 18: 450–458.
Ottolenghi, C., 2005 Foxl2 is required for commitment to ovary differentiation. Hum. Mol. Genet. 14: 2053–2062.
Ottolenghi, C., E. Pelosi, J. Tran, M. Colombino, E. Douglass *et al.*, 2007 Loss of Wnt4 and Foxl2 leads to female-to-male sex reversal extending to germ cells. Hum. Mol. Genet. 16: 2795–2804.
Pailhoux, E., B. Vigier, S. Chaffaux, N. Servel, S. Taourit *et al.*, 2001 A 11.7-kb deletion triggers intersexuality and polledness in goats. Nat. Genet. 29: 453–458.

Pal, L., and N. Santoro, 2002 Premature ovarian failure (POF): discordance between somatic and reproductive aging. Ageing Res. Rev. 1: 413–423.

Payne, A. H., and D. B. Hales, 2004 Overview of steroidogenic enzymes in the pathway from cholesterol to active steroid hormones. Endocr. Rev. 25: 947–970.

Raymond, C. S., M. W. Murphy, M. G. O'Sullivan, V. J. Bardwell, and D. Zarkower, 2000 Dmrt1, a gene related to worm and fly sexual regulators, is required for mammalian testis differentiation. Genes Dev. 14: 2587–2595.

Rodríguez-Marí, A., Y. L. Yan, R. A. BreMiller, C. Wilson, C. Cañestro *et al.*, 2005 Characterization and expression pattern of zebrafish anti-Müllerian hormone (amh) relative to sox9a, sox9b, and cyp19a1a, during gonad development. Gene Expr. Patterns 5: 655–667.

Rouiller-Fabre, V., S. Carmona, R. Abou Merhi, R. Cate, R. Habert *et al.*, 1998 Effect of anti-mullerian hormone on sertoli and leydig cell functions in fetal and immature rats. Endocrinology 139: 1213–1220.

Saito, D., C. Morinaga, Y. Aoki, S. Nakamura, H. Mitani *et al.*, 2007 Proliferation of germ cells during gonadal sex differentiation in medaka: insights from germ cell-depleted mutant zenzai. Dev. Biol. 310: 280–290.

Schmidt, D., 2004 The murine winged-helix transcription factor Foxl2 is required for granulosa cell differentiation and ovary maintenance. Development 131: 933–942.

Schulz, R. W., H. F. Vischer, J. E. B. Cavaco, E. M. Santos, C. R. Tyler *et al.*, 2001 Gonadotropins, their receptors, and the regulation of testicular functions in fish. Comp. Biochem. Physiol. B Biochem. Mol. Biol. 129: 407–417.

Sekido, R., and R. Lovell-Badge, 2008 Sex determination involves synergistic action of SRY and SF1 on a specific Sox9 enhancer. Nature 453: 930–934.

Shinomiya, A., M. Tanaka, T. Kobayashi, Y. Nagahama, and S. Hamaguchi, 2000 The vasa-like gene, olvas, identifies the migration path of primordial germ cells during embryonic body formation stage in the medaka, Oryzias latipes. Dev. Growth Differ. 42: 317–326.

Siegfried, K. R., 2010 In search of determinants: gene expression during gonadal sex differentiation. J. Fish Biol. 76: 1879–1902.

Siegfried, K. R., and C. Nüsslein-Volhard, 2008 Germ line control of female sex determination in zebrafish. Dev. Biol. 324: 277–287.

Smith, C. A., K. N. Roeszler, T. Ohnesorg, D. M. Cummins, P. G. Farlie *et al.*, 2009 The avian Z-linked gene DMRT1 is required for male sex determination in the chicken. Nature 461: 267–271.

Smith, E. K., J. M. Guzmán, and J. A. Luckenbach, 2013 Molecular cloning, characterization, and sexually dimorphic expression of five major sex differentiation-related genes in a Scorpaeniform fish, sablefish (*Anoplopoma fimbria*). Comp. Biochem. Physiol. B Biochem. Mol. Biol. 165: 125–137.

Sola, L., and E. Gornung, 2001 Classical and molecular cytogenetics of the zebrafish, *Danio rerio* (*Cyprinidae*, *Cypriniformes*): an overview. Genetica 111: 397–412.

Sreenivasan, R., M. N. Cai, R. Bartfai, X. G. Wang, A. Christoffels *et al.*, 2008 Transcriptomic analyses reveal novel genes with sexually dimorphic expression in the zebrafish gonad and brain. PLoS One 3: e1791.

Sridevi, P., and B. Senthilkumaran, 2011 Cloning and differential expression of FOXL2 during ovarian development and recrudescence of the catfish, *Clarias gariepinus*. Gen. Comp. Endocrinol. 174: 259–268.

Sridevi, P., R. K. Chaitanya, A. Dutta-Gupta, and B. Senthilkumaran, 2012 FTZ-F1 and FOXL2 up-regulate catfish brain aromatase gene transcription by specific binding to the promoter motifs. Biochim. Biophys. Acta 1819: 57–66.

Stahl, Y., and R. Simon, 2010 mRNA detection by whole mount in situ hybridization (WISH) or sectioned tissue in situ hybridization (SISH) in *Arabidopsis*. Methods Mol. Biol. 655: 239–251.

Stoilov, I., 2001 Cytochrome P450s: coupling development and environment. Trends Genet. 17: 629–632.

Sun, D., Y. Zhang, C. Wang, X. Hua, X. A. Zhang *et al.*, 2013 Sox9-related signaling controls zebrafish juvenile ovary-testis transformation. Cell Death Dis. 4: e930.

Takehana, Y., M. Matsuda, T. Myosho, M. L. Suster, K. Kawakami *et al.*, 2014 Co-option of Sox3 as the male-determining factor on the Y chromosome in the fish *Oryzias dancena*. Nat. Commun. 5: 4157.

Takahashi, H., 1976 Juvenile hermaphroditism in the zebrafish, *Brachydanio rerio*. J. Phys. Soc. Jpn. 41: 958–964.

Tamura, K., D. Peterson, N. Peterson, G. Stecher, M. Nei *et al.*, 2011 MEGA5: molecular evolutionary genetics analysis using maximum likelihood, evolutionary distance, and maximum parsimony methods. Mol. Biol. Evol. 28: 2731–2739.

Tevosian, S. G., K. H. Albrecht, J. D. Crispino, Y. Fujiwara, E. M. Eicher *et al.*, 2002 Gonadal differentiation, sex determination and normal Sry expression in mice require direct interaction between transcription partners GATA4 and FOG2. Development 129: 4627–4634.

Trant, J. M., S. Gavasso, J. Ackers, B. C. Chung, and A. R. Place, 2001 Developmental expression of cytochrome P450 aromatase genes (CYP19a and CYP19b) in zebrafish fry (*Danio rerio*). J. Exp. Zool. 290: 475–483.

Turola, E., S. Petta, E. Vanni, F. Milosa, L. Valenti *et al.*, 2015 Ovarian senescence increases liver fibrosis in humans and zebrafish with steatosis. Dis. Model. Mech. 8: 1037–1046.

Uchida, D., M. Yamashita, T. Kitano, and T. Iguchi, 2002 Oocyte apoptosis during the transition from ovary-like tissue to testes during sex differentiation of juvenile zebrafish. J. Exp. Biol. 205: 711–718.

Uda, M., C. Ottolenghi, L. Crisponi, J. E. Garcia, M. Deiana *et al.*, 2004 Foxl2 disruption causes mouse ovarian failure by pervasive blockage of follicle development. Hum. Mol. Genet. **13**: 1171–1181.

Uhlenhaut, N. H., S. Jakob, K. Anlag, T. Eisenberger, R. Sekido *et al.*, 2009 Somatic sex reprogramming of adult ovaries to testes by FOXL2 ablation. Cell 139: 1130–1142.

Vandesompele, J., K. De Preter, F. Pattyn, B. Poppe, N. Van Roy *et al.*, 2002 Accurate normalization of real-time quantitative RT-PCR data by geometric averaging of multiple internal control genes. Genome Biol. 3: RESEARCH0034.

Volff, J. N., I. Nanda, M. Schmid, and M. Schartl, 2007 Governing sex determination in fish: regulatory putsches and ephemeral dictators. Sex Dev. 1: 85–99.

Von Hofsten, J., and P. E. Olsson, 2005 Zebrafish sex determination and differentiation: involvement of FTZ-F1 genes. Reprod. Biol. Endocrinol. 3: 63.

Von Hofsten, J., A. Larsson, and P. E. Olsson, 2005a Novel steroidogenic factor-1 homolog (ff1d) is coexpressed with antimullerian hormone (amh) in zebrafish. Dev. Dyn. 233: 595–604.

Von Hofsten, J., C. Modig, A. Larsson, J. Karlsson, and P. E. Olsson, 2005b Determination of the expression pattern of the dual promoter of zebrafish fushi tarazu factor-1a following microinjections into zebrafish one cell stage embryos. Gen. Comp. Endocrinol. 142: 222–226.

Von Schalburg, K. R., M. Yasuike, W. S. Davidson, and B. F. Koop, 2010 Regulation, expression and characterization of aromatase (cyp19b1) transcripts in ovary and testis of rainbow trout (*Oncorhynchus mykiss*). Comp. Biochem. Physiol. B Biochem. Mol. Biol. 155: 118–125.

Wang, D. S., T. Kobayashi, L. Zhou, and Y. Nagahama, 2004 Molecular cloning and gene expression of Foxl2 in the Nile tilapia, *Oreochromis niloticus*. Biochem. Biophys. Res. Commun. 320: 83–89.

Wang, D. S., T. Kobayashi, L. Y. Zhou, B. Paul-Prasanth, S. Ijiri *et al.*, 2007 Foxl2 up-regulates aromatase gene transcription in a female-specific manner by binding to the promoter as well as interacting with Ad4 binding protein/steroidogenic factor 1. Mol. Endocrinol. 21: 712–725.

Wang, H., T. Wu, F. Qin, L. Wang, and Z. Wang, 2012 Molecular cloning of Foxl2 gene and the effects of endocrine-disrupting chemicals on its mRNA level in rare minnow, *Gobiocypris rarus*. Fish Physiol. Biochem. 38: 653–664.

Weigel, D., G. Jurgens, F. Kuttner, E. Seifert, and H. Jackle, 1989 The homeotic gene fork head encodes a nuclear-protein and is expressed in the terminal regions of the drosophila embryo. Cell 57: 645–658.

Westerfield, M., 2007 *The Zebrafish Book: A Guide for the Laboratory use of Zebrafish (Danio rerio)*, Ed. 5. University of Oregon Press, Eugene, OR.

Williams, T. M., and S. B. Carroll, 2009 Genetic and molecular insights into the development and evolution of sexual dimorphism. Nat. Rev. Genet. 10: 797–804.

Wilson, C. A., S. K. High, B. M. McCluskey, A. Amores, Y. L. Yan *et al.*, 2014 Wild sex in zebrafish: loss of the natural sex determinant in domesticated strains. Genetics 198: 1291–1308.

Wotton, K. R., K. E. M. French, and S. M. Shimeld, 2007 The developmental expression of foxl2 in the dogfish *Scyliorhinus canicula*. Gene Expr. Patterns 7: 793–797.

Wu, G. C., S. Tomy, M. Nakamura, and C. F. Chang, 2008 Dual roles of cyp19a1a in gonadal sex differentiation and development in the protandrous black porgy, *Acanthopagrus schlegeli*. Biol. Reprod. 79: 1111–1120.

Xia, W., L. Zhou, B. Yao, C. J. Li, and J. F. Gui, 2007 Differential and spermatogenic cell-specific expression of DMRT1 during sex reversal in protogynous hermaphroditic groupers. Mol. Cell. Endocrinol. 263: 156–172.

Xiong, S., J. Wu, J. Jing, P. Huang, Z. Li *et al.*, 2017 Loss of stat3 function leads to spine malformation and immune disorder in zebrafish. Sci. Bull. 62: 185–196.

Yamaguchi, T., S. Yamaguchi, T. Hirai, and T. Kitano, 2007 Follicle-stimulating hormone signaling and Foxl2 are involved in transcriptional regulation of aromatase gene during gonadal sex differentiation in Japanese flounder, *Paralichthys olivaceus*. Biochem. Biophys. Res. Commun. 359: 935–940.

Yano, A., R. Guyomard, B. Nicol, E. Jouanno, E. Quillet *et al.*, 2012 An immune-related gene evolved into the master sex-determining gene in rainbow trout, *Oncorhynchus mykiss*. Curr. Biol. 22: 1423–1428.

Yin, J., J. H. Xia, X. Z. Du, J. Liu, L. Zhou *et al.*, 2007 Developmental expression of CagMdkb during gibel carp embryogenesis. Int. J. Dev. Biol. 51: 761–769.

Yoshimoto, S., E. Okada, H. Umemoto, K. Tamura, Y. Uno *et al.*, 2008 A W-linked DM-domain gene, DM-W, participates in primary ovary development in *Xenopus laevis*. Proc. Natl. Acad. Sci. USA 105: 2469–2474.

Communicating editor: D. M. Parichy

GENETICS

Supporting Information
www.genetics.org/lookup/suppl/doi:10.1534/genetics.116.199133/-/DC1

Sequential, Divergent, and Cooperative Requirements of *Foxl2a* and *Foxl2b* in Ovary Development and Maintenance of Zebrafish

Yan-Jing Yang, Yang Wang, Zhi Li, Li Zhou and Jian-Fang Gui

DOI: 10.1534/genetics.116.199133